THE CONFRONTATION BETWEEN GENERAL RELATIVITY AND EXPERIMENT: A 1998 UPDATE

Clifford M. Will*
McDonnell Center for the Space Sciences
Department of Physics
Washington University, St. Louis MO 63130

ABSTRACT

The status of experimental tests of general relativity and of theoretical frameworks for analysing them are reviewed. Einstein's equivalence principle (EEP) is well supported by experiments such as the Eötvös experiment, tests of special relativity, and the gravitational redshift experiment. Future tests of EEP will search for new interactions arising from unification or quantum gravity. Tests of general relativity have reached high precision, including the light deflection, the Shapiro time delay, the perihelion advance of Mercury, and the Nordtvedt effect in lunar motion. Gravitational wave damping has been detected to half a percent using the binary pulsar, and new binary pulsar systems promise further improvements. When direct observation of gravitational radiation from astrophysical sources begins, new tests of general relativity will be possible.

*Support in part by NSF Grant 96-00049

© 1998 by Clifford M. Will.

1 Introduction

At the time of the birth of general relativity (GR), experimental confirmation was almost a side issue. Einstein did calculate observable effects of general relativity, such as the deflection of light, which were tested, but compared to the inner consistency and elegance of the theory, he regarded such empirical questions as almost peripheral. But today, experimental gravitation is a major component of the field, characterized by continuing efforts to test the theory's predictions, to search for gravitational imprints of high-energy particle interactions, and to detect gravitational waves from astronomical sources.

The modern history of experimental relativity can be divided roughly into four periods, Genesis, Hibernation, a Golden Era, and the Quest for Strong Gravity. The Genesis (1887–1919) comprises the period of the two great experiments which were the foundation of relativistic physics—the Michelson-Morley experiment and the Eötvös experiment—and the two immediate confirmations of GR—the deflection of light and the perihelion advance of Mercury. Following this was a period of Hibernation (1920–1960) during which relatively few experiments were performed to test GR, and at the same time the field itself became sterile and stagnant, relegated to the backwaters of physics and astronomy.

But beginning around 1960, astronomical discoveries (quasars, pulsars, cosmic background radiation) and new experiments pushed GR to the forefront. Experimental gravitation experienced a Golden Era (1960–1980) during which a systematic, world-wide effort took place to understand the observable predictions of GR, to compare and contrast them with the predictions of alternative theories of gravity, and to perform new experiments to test them. The period began with an experiment to confirm the gravitational frequency shift of light (1960) and ended with the reported decrease in the orbital period of the binary pulsar at a rate consistent with the general relativity prediction of gravity-wave energy loss (1979). The results all supported GR, and most alternative theories of gravity fell by the wayside (for a popular review, see Ref. 1).

Since 1980, the field has entered what might be termed a Quest for Strong Gravity. Many of the remaining interesting weak-field predictions of the theory are extremely small and difficult to check, in some cases requiring further technological development to bring them into detectable range. The sense of a systematic assault on the weak-field predictions of GR has been supplanted to some extent

by an opportunistic approach in which novel and unexpected (and sometimes inexpensive) tests of gravity have arisen from new theoretical ideas or experimental techniques, often from unlikely sources. Examples include the use of laser-cooled atom and ion traps to perform ultra-precise tests of special relativity, and the startling proposal of a "fifth" force, which led to a host of new tests of gravity at short ranges. Several major ongoing efforts also continue, principally the Stanford Gyroscope experiment, known as Gravity Probe-B.

Instead, much of the focus has shifted to experiments which can probe the effects of strong gravitational fields. At one extreme are the strong gravitational fields associated with Planck-scale physics. Will unification of the forces, or quantization of gravity at this scale leave observable effects accessible by experiment? Dramatically improved tests of the equivalence principle or of the "inverse square law" are being designed, to search for or bound the imprinted effects of Planck scale phenomena. At the other extreme are the strong fields associated with compact objects such as black holes or neutron stars. Astrophysical observations and gravitational-wave detectors are being planned to explore and test GR in the strong-field, highly-dynamical regime associated with the formation and dynamics of these objects.

In these lectures, we shall review theoretical frameworks for studying experimental gravitation, summarize the current status of experiments, and attempt to chart the future of the subject. We shall not provide complete references to work done in this field but instead will refer the reader to the appropriate review articles and monographs, specifically to *Theory and Experiment in Gravitational Physics*,[2] hereafter referred to as TEGP. Additional recent reviews in this subject are Refs. 3, 4, 5 and 6. Other references will be confined to reviews or monographs on specific topics, and to important recent papers that are not included in TEGP. References to TEGP will be by chapter or section, *e.g.* "TEGP 8.9".

2 Tests of the Foundations of Gravitation Theory

2.1 The Einstein Equivalence Principle

The principle of equivalence has historically played an important role in the development of gravitation theory. Newton regarded this principle as such a cornerstone of mechanics that he devoted the opening paragraph of the *Principia* to it. In 1907, Einstein used the principle as a basic element of general relativity. We now regard the principle of equivalence as the foundation, not of Newtonian gravity or of GR, but of the broader idea that spacetime is curved.

One elementary equivalence principle is the kind Newton had in mind when he stated that the property of a body called "mass" is proportional to the "weight", and is known as the weak equivalence principle (WEP). An alternative statement of WEP is that the trajectory of a freely falling body (one not acted upon by such forces as electromagnetism and too small to be affected by tidal gravitational forces) is independent of its internal structure and composition. In the simplest case of dropping two different bodies in a gravitational field, WEP states that the bodies fall with the same acceleration.

A more powerful and far-reaching equivalence principle is known as the Einstein equivalence principle (EEP). It states that (i) WEP is valid, (ii) the outcome of any local non-gravitational experiment is independent of the velocity of the freely-falling reference frame in which it is performed, and (iii) the outcome of any local non-gravitational experiment is independent of where and when in the universe it is performed. The second piece of EEP is called local Lorentz invariance (LLI), and the third piece is called local position invariance (LPI).

For example, a measurement of the electric force between two charged bodies is a local non-gravitational experiment; a measurement of the gravitational force between two bodies (Cavendish experiment) is not.

The Einstein equivalence principle is the heart and soul of gravitational theory, for it is possible to argue convincingly that if EEP is valid, then gravitation must be a "curved spacetime" phenomenon, in other words, the effects of gravity must be equivalent to the effects of living in a curved spacetime. As a consequence of this argument, the only theories of gravity that can embody EEP are those that satisfy the postulates of "metric theories of gravity", which are (i) spacetime is

endowed with a symmetric metric, (ii) the trajectories of freely falling bodies are geodesics of that metric, and (iii) in local freely falling reference frames, the non-gravitational laws of physics are those written in the language of special relativity. The argument that leads to this conclusion simply notes that, if EEP is valid, then in local freely falling frames, the laws governing experiments must be independent of the velocity of the frame (local Lorentz invariance), with constant values for the various atomic constants (in order to be independent of location). The only laws we know of that fulfill this are those that are compatible with special relativity, such as Maxwell's equations of electromagnetism. Furthermore, in local freely falling frames, test bodies appear to be unaccelerated, in other words they move on straight lines; but such "locally straight" lines simply correspond to "geodesics" in a curved spacetime (TEGP 2.3).

General relativity is a metric theory of gravity, but then so are many others, including the Brans-Dicke theory. The nonsymmetric gravitation theory (NGT) of Moffat is not a metric theory, neither is superstring theory (see Sec. 2.3). So the notion of curved spacetime is a very general and fundamental one, and therefore it is important to test the various aspects of the Einstein Equivalence Principle thoroughly.

A direct test of WEP is the comparison of the acceleration of two laboratory-sized bodies of different composition in an external gravitational field. If the principle were violated, then the accelerations of different bodies would differ. The simplest way to quantify such possible violations of WEP in a form suitable for comparison with experiment is to suppose that for a body with inertial mass m_I, the passive gravitational mass m_P is no longer equal to m_I, so that in a gravitational field g, the acceleration is given by $m_I a = m_P g$. Now the inertial mass of a typical laboratory body is made up of several types of mass-energy: rest energy, electromagnetic energy, weak-interaction energy, and so on. If one of these forms of energy contributes to m_P differently than it does to m_I, a violation of WEP would result. One could then write

$$m_P = m_I + \sum_A \eta^A E^A / c^2 \,, \tag{1}$$

where E^A is the internal energy of the body generated by interaction A, and η^A is a dimensionless parameter that measures the strength of the violation of WEP induced by that interaction, and c is the speed of light. A measurement or limit on the fractional difference in acceleration between two bodies then yields a quantity

called the "Eötvös ratio" given by

$$\eta \equiv \frac{2|a_1 - a_2|}{|a_1 + a_2|} = \sum_A \eta^A \left(\frac{E_1^A}{m_1 c^2} - \frac{E_2^A}{m_2 c^2} \right) , \qquad (2)$$

where we drop the subscript I from the inertial masses. Thus, experimental limits on η place limits on the WEP-violation parameters η^A.

Many high-precision Eötvös-type experiments have been performed, from the pendulum experiments of Newton, Bessel and Potter, to the classic torsion-balance measurements of Eötvös, Dicke, Braginsky and their collaborators. In the modern torsion-balance experiments, two objects of different composition are connected by a rod or placed on a tray and suspended in a horizontal orientation by a fine wire. If the gravitational acceleration of the bodies differs, there will be a torque induced on the suspension wire, related to the angle between the wire and the direction of the gravitational acceleration $\mathbf{g}$. If the entire apparatus is rotated about some direction with angular velocity ω, the torque will be modulated with period $2\pi/\omega$. In the experiments of Eötvös and his collaborators, the wire and $\mathbf{g}$ were not quite parallel because of the centripetal acceleration on the apparatus due to the Earth's rotation; the apparatus was rotated about the direction of the wire. In the Princeton (Dicke *et al.*), and Moscow (Braginsky *et al.*) experiments, $\mathbf{g}$ was that of the Sun, and the rotation of the Earth provided the modulation of the torque at a period of 24 hr (TEGP 2.4(a)). Beginning in the late 1980s, numerous experiments were carried out primarily to search for a "fifth force" (see Sec. 2.3), but their null results also constituted tests of WEP. In the "free-fall Galileo experiment" performed at the University of Colorado, the relative free-fall acceleration of two bodies made of uranium and copper was measured using a laser interferometric technique. The "Eöt-Wash" experiment carried out at the University of Washington used a sophisticated torsion balance tray to compare the accelerations of beryllium and copper toward local topography on Earth, movable laboratory masses, the Sun and the galaxy.[7] The resulting upper limits on η are summarized in Figure 1 (TEGP 14.1; for a bibliography of experiments, see Ref. 8.

The second ingredient of EEP, local Lorentz invariance, can be said to be tested every time that special relativity is confirmed in the laboratory. However, many such experiments, especially in high-energy physics, are not "clean" tests, because in many cases it is unlikely that a violation of Lorentz invariance could be distinguished from effects due to the complicated strong and weak interactions.

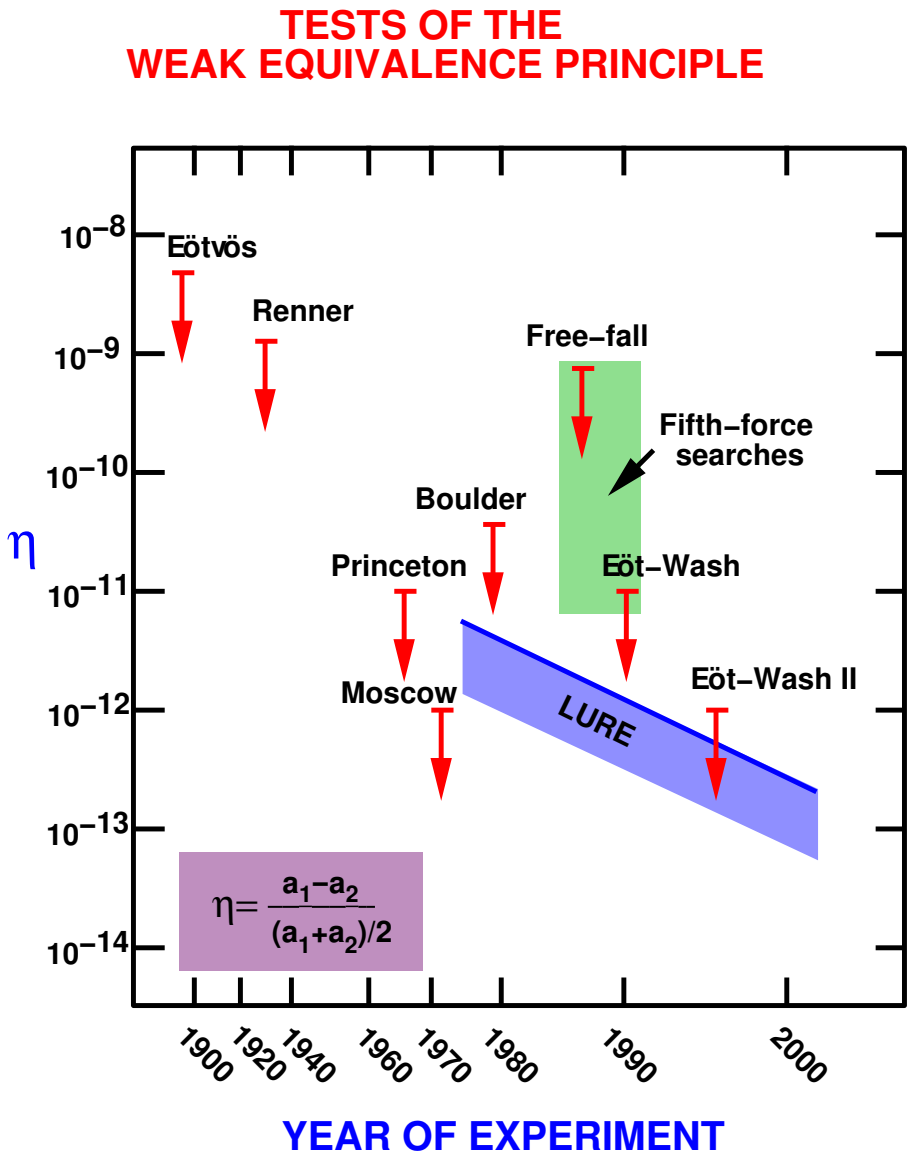

Fig. 1. Selected tests of the Weak Equivalence Principle, showing bounds on η, which measures fractional difference in acceleration of different materials or bodies. Free-fall and Eöt-Wash experiments originally performed to search for fifth force. Hatched line shows current bounds on η for gravitating bodies from lunar laser ranging (LURE).

However, there is one class of experiments that can be interpreted as "clean", high-precision tests of local Lorentz invariance. These are the "mass anisotropy" experiments: the classic versions are the Hughes-Drever experiments, performed in the period 1959-60 independently by Hughes and collaborators at Yale University, and by Drever at Glasgow University (TEGP 2.4(b)). Dramatically improved versions were carried out during the late 1980s using laser-cooled trapped atom techniques (TEGP 14.1). A simple and useful way of interpreting these experiments is to suppose that the electromagnetic interactions suffer a slight violation of Lorentz invariance, through a change in the speed of electromagnetic radiation c relative to the limiting speed of material test particles (c_0, chosen to be unity via a choice of units), in other words, $c \neq 1$ (see Sec. 2.2.3). Such a violation necessarily selects a preferred universal rest frame, presumably that of the cosmic background radiation, through which we are moving at about 300 km/s. Such a Lorentz-non-invariant electromagnetic interaction would cause shifts in the energy levels of atoms and nuclei that depend on the orientation of the quantization axis of the state relative to our universal velocity vector, and on the quantum numbers of the state. The presence or absence of such energy shifts can be examined by measuring the energy of one such state relative to another state that is either unaffected or is affected differently by the supposed violation. One way is to look for a shifting of the energy levels of states that are ordinarily equally spaced, such as the four J=3/2 ground states of the ^{7}Li nucleus in a magnetic field (Drever experiment); another is to compare the levels of a complex nucleus with the atomic hyperfine levels of a hydrogen maser clock. These experiments have all yielded extremely accurate results, quoted as limits on the parameter $\delta \equiv c^{-2} - 1$ in Figure 2. Also included for comparison is the corresponding limit obtained from Michelson-Morley type experiments.

Recent advances in atomic spectroscopy and atomic timekeeping have made it possible to test LLI by checking the isotropy of the speed of light using one-way propagation (as opposed to round-trip propagation, as in the Michelson-Morley experiment). In one experiment, for example, the relative phases of two hydrogen maser clocks at two stations of NASA 's Deep Space Tracking Network were compared over five rotations of the Earth by propagating a light signal one-way along an ultrastable fiberoptic link connecting them (see Sec. 2.2.3). Although the bounds from these experiments are not as tight as those from mass-anisotropy experiments, they probe directly the fundamental postulates of special relativity,

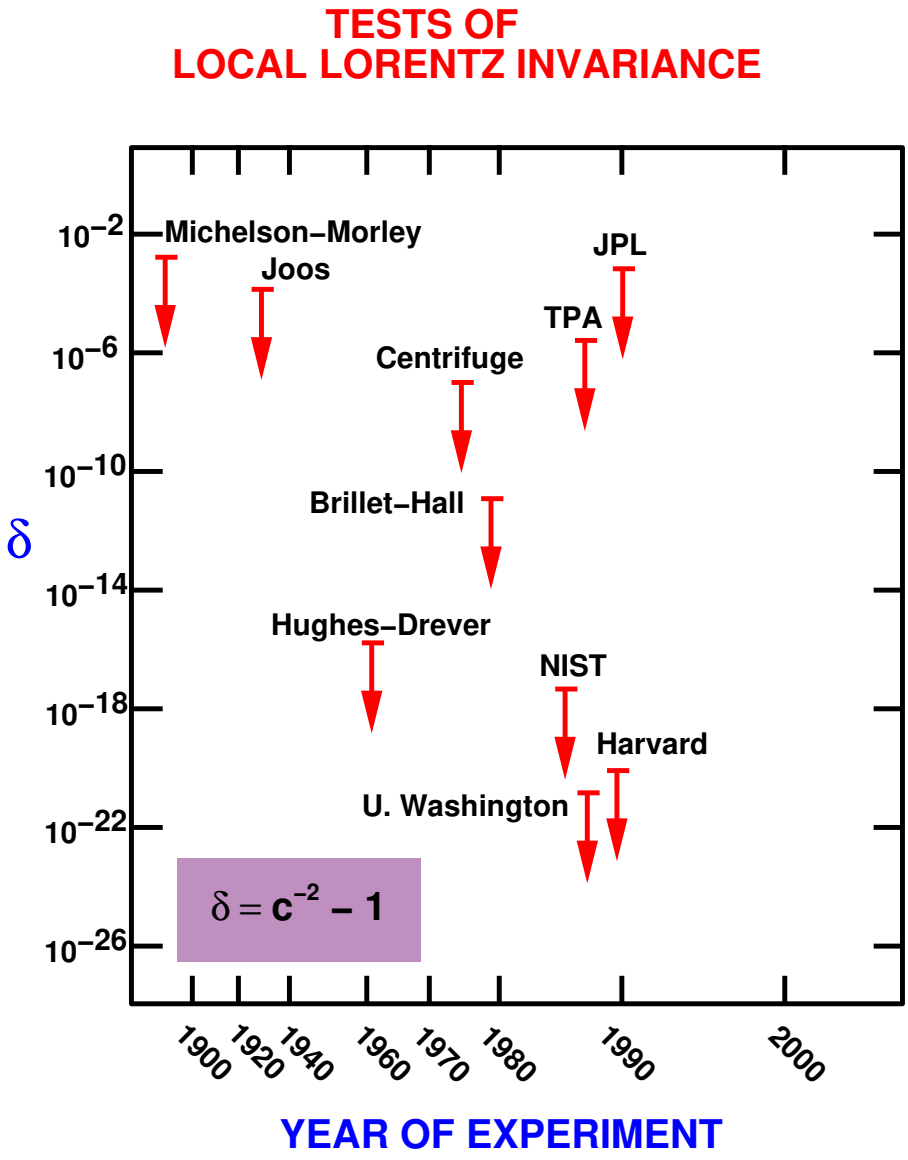

Fig. 2. Selected tests of local Lorentz invariance showing bounds on parameter δ, which measures degree of violation of Lorentz invariance in electromagnetism. Michelson-Morley, Joos, and Brillet-Hall experiments test isotropy of round-trip speed of light, the latter experiment using laser technology. Centrifuge, two-photon absorption (TPA) and JPL experiments test isotropy of light speed using one-way propagation. Remaining four experiments test isotropy of nuclear energy levels. Limits assume speed of Earth of 300 km/s relative to the mean rest frame of the universe.

and thereby of LLI. (TEGP 14.1).

The principle of local position invariance, the third part of EEP, can be tested by the gravitational redshift experiment, the first experimental test of gravitation proposed by Einstein. Despite the fact that Einstein regarded this as a crucial test of GR, we now realize that it does not distinguish between GR and any other metric theory of gravity, instead is a test only of EEP. A typical gravitational redshift experiment measures the frequency or wavelength shift $Z \equiv \Delta\nu/\nu = -\Delta\lambda/\lambda$ between two identical frequency standards (clocks) placed at rest at different heights in a static gravitational field. If the frequency of a given type of atomic clock is the same when measured in a local, momentarily comoving freely falling frame (Lorentz frame), independent of the location or velocity of that frame, then the comparison of frequencies of two clocks at rest at different locations boils down to a comparison of the velocities of two local Lorentz frames, one at rest with respect to one clock at the moment of emission of its signal, the other at rest with respect to the other clock at the moment of reception of the signal. The frequency shift is then a consequence of the first-order Doppler shift between the frames. The structure of the clock plays no role whatsoever. The result is a shift

$$Z = \Delta U/c^2\,, \tag{3}$$

where ΔU is the difference in the Newtonian gravitational potential between the receiver and the emitter. If LPI is not valid, then it turns out that the shift can be written

$$Z = (1+\alpha)\Delta U/c^2\,, \tag{4}$$

where the parameter α may depend upon the nature of the clock whose shift is being measured (see TEGP 2.4(c) for details).

The first successful, high-precision redshift measurement was the series of Pound-Rebka-Snider experiments of 1960-1965, that measured the frequency shift of gamma-ray photons from ^{57}Fe as they ascended or descended the Jefferson Physical Laboratory tower at Harvard University. The high accuracy achieved–one percent–was obtained by making use of the Mössbauer effect to produce a narrow resonance line whose shift could be accurately determined. Other experiments since 1960 measured the shift of spectral lines in the Sun's gravitational field and the change in rate of atomic clocks transported aloft on aircraft, rockets and satellites. Figure 3 summarizes the important redshift experiments that have been performed since 1960 (TEGP 2.4(c)).

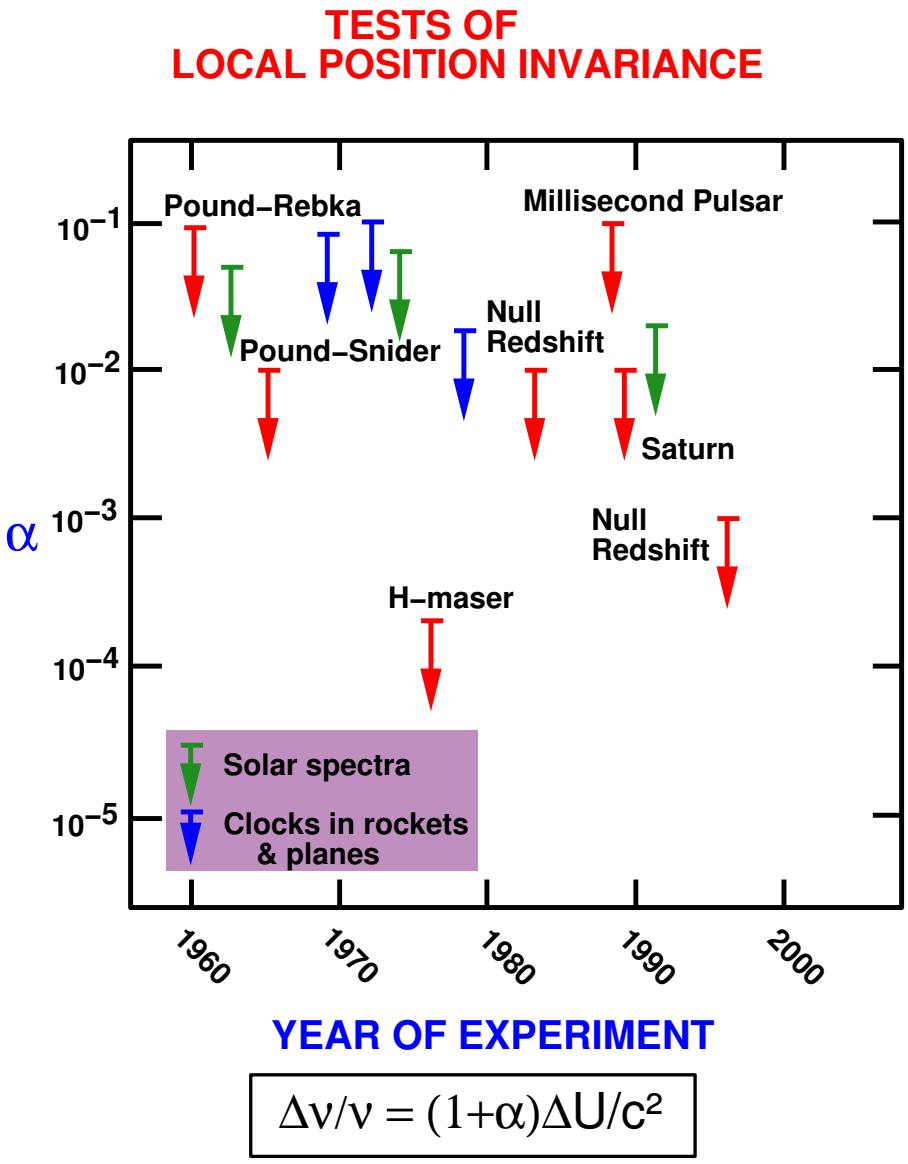

Fig. 3. Selected tests of local position invariance via gravitational redshift experiments, showing bounds on α, which measures degree of deviation of redshift from the formula $\Delta\nu/\nu = \Delta U/c^2$.

The most precise experiment to date was the Vessot-Levine rocket redshift experiment that took place in June 1976. A hydrogen-maser clock was flown on a rocket to an altitude of about 10,000 km and its frequency compared to a similar clock on the ground. The experiment took advantage of the masers' frequency stability by monitoring the frequency shift as a function of altitude. A sophisticated data acquisition scheme accurately eliminated all effects of the first-order Doppler shift due to the rocket's motion, while tracking data were used to determine the payload's location and the velocity (to evaluate the potential difference ΔU, and the special relativistic time dilation). Analysis of the data yielded a limit $|\alpha| < 2 \times 10^{-4}$.

A "null" redshift experiment performed in 1978 tested whether the *relative* rates of two different clocks depended upon position. Two hydrogen maser clocks and an ensemble of three superconducting-cavity stabilized oscillator (SCSO) clocks were compared over a 10-day period. During this period, the solar potential U/c^2 changed sinusoidally with a 24-hour period by 3×10^{-13} because of the Earth's rotation, and changed linearly at 3×10^{-12} per day because the Earth is 90 degrees from perihelion in April. However, analysis of the data revealed no variations of either type within experimental errors, leading to a limit on the LPI violation parameter $|\alpha^{\rm H} - \alpha^{\rm SCSO}| < 2 \times 10^{-2}$. This bound is likely to be improved using more stable frequency standards.[9,10] The varying gravitational redshift of Earth-bound clocks relative to the highly stable Millisecond Pulsar, caused by the Earth's motion in the solar gravitational field around the Earth-Moon center of mass (amplitude 4000 km), has been measured to about 10 percent, and the redshift of stable oscillator clocks on the Voyager spacecraft caused by Saturn's gravitational field yielded a one percent test. The solar gravitational redshift has been tested to about two percent using infrared oxygen triplet lines at the limb of the Sun, and to one percent using oscillator clocks on the Galileo spacecraft (TEGP 2.4(c) and 14.1(a)).

Modern advances in navigation using Earth-orbiting atomic clocks and accurate time-transfer must routinely take gravitational redshift and time-dilation effects into account. For example, the Global Positioning System (GPS) provides absolute accuracies of around 15 m (even better in its military mode) anywhere on Earth, which corresponds to 50 nanoseconds in time accuracy at all times. Yet the difference in rate between satellite and ground clocks as a result of special and general relativistic effects is a whopping 40 *microseconds* per day (60μs from the

Constant k	Limit on $\dot{k}/k$ per Hubble time 1.2×10^{10}yr	Method
Fine structure constant $\alpha = e^2/\hbar c$	4×10^{-4}	H-maser vs Hg ion clock[10]
	6×10^{-7}	Oklo Natural Reactor[11]
	6×10^{-5}	21-cm vs molecular absorption at $Z = 0.7$ (Ref. 12)
Weak interaction constant $\beta = G_f m_p^2 c/\hbar^3$	1	^{187}Re, ^{40}K decay rates
	0.1	Oklo Natural Reactor[11]
	0.06	Big bang nucleosynthesis[13]
e-p mass ratio	1	Mass shift in quasar spectra at $Z \sim 2$
Proton g-factor (g_p)	10^{-5}	21-cm vs molecular absorption at $Z = 0.7$ (Ref. 12)

Table 1. Bounds on cosmological variation of fundamental constants of non-gravitational physics. For references to earlier work, see TEGP 2.4(c).

gravitational redshift, and $-20\,\mu$s from time dilation). If these effects were not accurately accounted for, GPS would fail to function at its stated accuracy. This represents a welcome practical application of GR!

Local position invariance also refers to position in time. If LPI is satisfied, the fundamental constants of non-gravitational physics should be constants in time. Table 1 shows current bounds on cosmological variations in selected dimensionless constants. For discussion and references to early work, see TEGP 2.4(c).

2.2 Theoretical Frameworks for Analyzing EEP

2.2.1 Schiff's Conjecture

Because the three parts of the Einstein equivalence principle discussed above are so very different in their empirical consequences, it is tempting to regard them as independent theoretical principles. On the other hand, any complete and self-consistent gravitation theory must possess sufficient mathematical machinery to

make predictions for the outcomes of experiments that test each principle, and because there are limits to the number of ways that gravitation can be meshed with the special relativistic laws of physics, one might not be surprised if there were theoretical connections between the three sub-principles. For instance, the same mathematical formalism that produces equations describing the free fall of a hydrogen atom must also produce equations that determine the energy levels of hydrogen in a gravitational field, and thereby the ticking rate of a hydrogen maser clock. Hence a violation of EEP in the fundamental machinery of a theory that manifests itself as a violation of WEP might also be expected to show up as a violation of local position invariance. Around 1960, Schiff conjectured that this kind of connection was a necessary feature of any self-consistent theory of gravity. More precisely, Schiff's conjecture states that *any complete, self-consistent theory of gravity that embodies WEP necessarily embodies EEP*. In other words, the validity of WEP alone guarantees the validity of local Lorentz and position invariance, and thereby of EEP.

If Schiff's conjecture is correct, then Eötvös experiments may be seen as the direct empirical foundation for EEP, hence for the interpretation of gravity as a curved-spacetime phenomenon. Of course, a rigorous proof of such a conjecture is impossible (indeed, some special counter-examples are known) yet a number of powerful "plausibility" arguments can be formulated.

The most general and elegant of these arguments is based upon the assumption of energy conservation. This assumption allows one to perform very simple cyclic gedanken experiments in which the energy at the end of the cycle must equal that at the beginning of the cycle. This approach was pioneered by Dicke, Nordtvedt and Haugan. A system in a quantum state A decays to state B, emitting a quantum of frequency ν. The quantum falls a height H in an external gravitational field and is shifted to frequency ν', while the system in state B falls with acceleration g_B. At the bottom, state A is rebuilt out of state B, the quantum of frequency ν', and the kinetic energy $m_B g_B H$ that state B has gained during its fall. The energy left over must be exactly enough, $m_A g_A H$, to raise state A to its original location. (Here an assumption of local Lorentz invariance permits the inertial masses m_A and m_B to be identified with the total energies of the bodies.) If g_A and g_B depend on that portion of the internal energy of the states that was

involved in the quantum transition from A to B according to

$$g_A = g(1 + \alpha E_A/m_A c^2)\,, \qquad g_B = g(1 + \alpha E_B/m_B c^2)\,, \qquad E_A - E_B \equiv h\nu \quad (5)$$

(violation of WEP), then by conservation of energy, there must be a corresponding violation of LPI in the frequency shift of the form (to lowest order in $h\nu/mc^2$)

$$Z = (\nu' - \nu)/\nu' = (1 + \alpha)gH/c^2 = (1 + \alpha)\Delta U/c^2\,. \quad (6)$$

Haugan generalized this approach to include violations of LLI (TEGP 2.5).

2.2.2 The $TH\epsilon\mu$ Formalism

The first successful attempt to prove Schiff's conjecture more formally was made by Lightman and Lee. They developed a framework called the $TH\epsilon\mu$ formalism that encompasses all metric theories of gravity and many non-metric theories (Box 1). It restricts attention to the behavior of charged particles (electromagnetic interactions only) in an external static spherically symmetric (SSS) gravitational field, described by a potential U. It characterizes the motion of the charged particles in the external potential by two arbitrary functions $T(U)$ and $H(U)$, and characterizes the response of electromagnetic fields to the external potential (gravitationally modified Maxwell equations) by two functions $\epsilon(U)$ and $\mu(U)$. The forms of T, H, ϵ and μ vary from theory to theory, but every metric theory satisfies

$$\epsilon = \mu = (H/T)^{1/2}\,, \quad (7)$$

for all U. This consequence follows from the action of electrodynamics with a "minimal" or metric coupling:

$$\begin{aligned} I &= -\sum_a m_{0a} \int (g_{\mu\nu} v_a^\mu v_a^\nu)^{1/2} dt + \sum_a e_a \int A_\mu(x_a^\nu) v_a^\mu dt \\ &- \frac{1}{16\pi} \int \sqrt{-g} g^{\mu\alpha} g^{\nu\beta} F_{\mu\nu} F_{\alpha\beta} d^4x\,, \end{aligned} \quad (8)$$

where the variables are defined in Box 1, and where $F_{\mu\nu} \equiv A_{\nu,\mu} - A_{\mu,\nu}$. By identifying $g_{00} = T$ and $g_{ij} = H\delta_{ij}$ in a SSS field, $F_{i0} = E_i$ and $F_{ij} = \epsilon_{ijk} B_k$, one obtains Equation 7.

Conversely, every theory within this class that satisfies Equation 7 can have its electrodynamic equations cast into "metric" form. Lightman and Lee then calculated explicitly the rate of fall of a "test" body made up of interacting charged

Box 1. The $TH\epsilon\mu$ Formalism

1. **Coordinate System and Conventions:**

   $x^0 = t$ = time coordinate associated with the static nature of the static spherically symmetric (SSS) gravitational field; $\mathbf{x} = (x, y, z)$ = isotropic quasi-Cartesian spatial coordinates; spatial vector and gradient operations as in Cartesian space.

2. **Matter and Field Variables:**

   - m_{0a} = rest mass of particle a.
   - e_a = charge of particle a.
   - $x_a^\mu(t)$ = world line of particle a.
   - $v_a^\mu = dx_a^\mu/dt$ = coordinate velocity of particle a.
   - A_μ = electromagnetic vector potential; $\mathbf{E} = \nabla A_0 - \partial\mathbf{A}/\partial t$, $\mathbf{B} = \nabla \times \mathbf{A}$

3. **Gravitational Potential:** $U(\mathbf{x})$

4. **Arbitrary Functions:**

   $T(U)$, $H(U)$, $\epsilon(U)$, $\mu(U)$; EEP is satisfied iff $\epsilon = \mu = (H/T)^{1/2}$ for all U.

5. **Action:**

$$I = -\sum_a m_{0a} \int (T - H v_a^2)^{1/2} dt + \sum_a e_a \int A_\mu(x_a^\nu) v_a^\mu dt + (8\pi)^{-1} \int (\epsilon E^2 - \mu^{-1} B^2) d^4x \,.$$

6. **Non-Metric Parameters:**

$$\begin{aligned} \Gamma_0 &= -c_0^2 (\partial/\partial U) \ln[\epsilon (T/H)^{1/2}]_0 \,, \\ \Lambda_0 &= -c_0^2 (\partial/\partial U) \ln[\mu (T/H)^{1/2}]_0 \,, \\ \Upsilon_0 &= 1 - (T H^{-1} \epsilon\mu)_0 \,, \end{aligned}$$

   where $c_0 = (T_0/H_0)^{1/2}$ and subscript "0" refers to a chosen point in space. If EEP is satisfied, $\Gamma_0 \equiv \Lambda_0 \equiv \Upsilon_0 \equiv 0$.

particles, and found that the rate was independent of the internal electromagnetic structure of the body (WEP) if and only if Equation 7 was satisfied. In other words WEP $\rightarrow$ EEP and Schiff's conjecture was verified, at least within the restrictions built into the formalism.

Certain combinations of the functions T, H, ϵ and μ reflect different aspects of EEP. For instance, position or U-dependence of either of the combinations $\epsilon(T/H)^{1/2}$ and $\mu(T/H)^{1/2}$ signals violations of LPI, the first combination playing the role of the locally measured electric charge or fine structure constant. The "non-metric parameters" Γ_0 and Λ_0 (Box 1) are measures of such violations of EEP. Similarly, if the parameter $\Upsilon_0 \equiv 1 - (TH^{-1}\epsilon\mu)_0$ is non-zero anywhere, then violations of LLI will occur. This parameter is related to the difference between the speed of light, c, and the limiting speed of material test particles, c_o, given by

$$c = (\epsilon_0\mu_0)^{-1/2}\,, \qquad c_o \;=\; (T_0/H_0)^{1/2}\,. \tag{9}$$

In many applications, by suitable definition of units, c_0 can be set equal to unity. If EEP is valid, $\Gamma_0 \equiv \Lambda_0 \equiv \Upsilon_0 = 0$ everywhere.

The rate of fall of a composite spherical test body of electromagnetically interacting particles then has the form

$$\mathbf{a} \;=\; (m_P/m)\nabla U\,, \tag{10}$$

$$m_P/m \;=\; 1 + (E_B^{ES}/Mc_0^2)[2\Gamma_0 - \frac{8}{3}\Upsilon_0] + (E_B^{MS}/Mc_0^2)[2\Lambda_0 - \frac{4}{3}\Upsilon_0] + \ldots, \tag{11}$$

where E_B^{ES} and E_B^{MS} are the electrostatic and magnetostatic binding energies of the body, given by

$$E_B^{ES} \;=\; -\frac{1}{4}T_0^{1/2}H_0^{-1}\epsilon_0^{-1}\left\langle \sum_{ab} e_a e_b r_{ab}^{-1} \right\rangle\,, \tag{12}$$

$$E_B^{MS} \;=\; -\frac{1}{8}T_0^{1/2}H_0^{-1}\mu_0\left\langle \sum_{ab} e_a e_b r_{ab}^{-1}[\mathbf{v}_a\cdot\mathbf{v}_b + (\mathbf{v}_a\cdot\mathbf{n}_{ab})(\mathbf{v}_b\cdot\mathbf{n}_{ab})] \right\rangle\,, \tag{13}$$

where $r_{ab} = |\mathbf{x}_a - \mathbf{x}_b|$, $\mathbf{n}_{ab} = (\mathbf{x}_a - \mathbf{x}_b)/r_{ab}$, and the angle brackets denote an expectation value of the enclosed operator for the system's internal state. Eötvös experiments place limits on the WEP-violating terms in Equation 11, and ultimately place limits on the non-metric parameters $|\Gamma_0| < 2\times10^{-10}$ and $|\Lambda_0| < 3\times10^{-6}$. (We set $\Upsilon_0 = 0$ because of very tight constraints on it from tests of LLI .) These limits are sufficiently tight to rule out a number of non-metric theories of gravity thought previously to be viable (TEGP 2.6(f)).

The $TH\epsilon\mu$ formalism also yields a gravitationally modified Dirac equation that can be used to determine the gravitational redshift experienced by a variety of atomic clocks. For the redshift parameter α (Equation 4), the results are (TEGP 2.6(c))

$$\alpha = \begin{cases} -3\Gamma_0 + \Lambda_0 & \text{hydrogen hyperfine transition, H} - \text{Maser clock} \\ -\frac{1}{2}(3\Gamma_0 + \Lambda_0) & \text{electromagnetic mode in cavity, SCSO clock} \\ -2\Gamma_0 & \text{phonon mode in solid, principal transition in hydrogen.} \end{cases} \tag{14}$$

The redshift is the standard one ($\alpha = 0$), independently of the nature of the clock if and only if $\Gamma_0 \equiv \Lambda_0 \equiv 0$. Thus the Vessot-Levine rocket redshift experiment sets a limit on the parameter combination $|3\Gamma_0 - \Lambda_0|$ (Figure 3); the null-redshift experiment comparing hydrogen-maser and SCSO clocks sets a limit on $|\alpha_H - \alpha_{SCSO}| = \frac{3}{2}|\Gamma_0 - \Lambda_0|$.

2.2.3 The c^2 Formalism

The $TH\epsilon\mu$ formalism can also be applied to tests of local Lorentz invariance, but in this context it can be simplified. Since most such tests do not concern themselves with the spatial variation of the functions T, H, ϵ, and μ, but rather with observations made in moving frames, we can treat them as spatial constants. Then by rescaling the time and space coordinates, the charges and the electromagnetic fields, we can put the action in Box 1 into the form (TEGP 2.6(a)).

$$I = -\sum_a m_{0a} \int (1 - v_a^2)^{1/2} dt + \sum_a e_a \int A_\mu(x_a^\nu) v_a^\mu dt + (8\pi)^{-1} \int (E^2 - c^2 B^2) d^4x \,, \tag{15}$$

where $c^2 \equiv H_0/T_0\epsilon_0\mu_0 = (1 - \Upsilon_0)^{-1}$. This amounts to using units in which the limiting speed c_o of massive test particles is unity, and the speed of light is c. If $c \neq 1$, LLI is violated; furthermore, the form of the action above must be assumed to be valid only in some preferred universal rest frame. The natural candidate for such a frame is the rest frame of the microwave background.

The electrodynamical equations which follow from Equation 15 yield the behavior of rods and clocks, just as in the full $TH\epsilon\mu$ formalism. For example, the length of a rod moving through the rest frame in a direction parallel to its length will be observed by a rest observer to be contracted relative to an identical rod perpendicular to the motion by a factor $1 - V^2/2 + O(V^4)$. Notice that c does not appear in this expression. The energy and momentum of an electromagnetically

bound body which moves with velocity $\mathbf{V}$ relative to the rest frame are given by

$$\begin{aligned} E &= M_R + \frac{1}{2}M_R V^2 + \frac{1}{2}\delta M_I^{ij} V^i V^j \,, \\ P^i &= M_R V^i + \delta M_I^{ij} V^j \,, \end{aligned} \tag{16}$$

where $M_R = M_0 - E_B^{ES}$, M_0 is the sum of the particle rest masses, E_B^{ES} is the electrostatic binding energy of the system (Equation 12 with $T_0^{1/2} H_0 \epsilon_0^{-1} = 1$), and

$$\delta M_I^{ij} = -2(\frac{1}{c^2} - 1)[\frac{4}{3}E_B^{ES}\delta^{ij} + \tilde{E}_B^{ESij}] \,, \tag{17}$$

where

$$\tilde{E}_B^{ESij} = -\frac{1}{4}\left\langle \sum_{ab} e_a e_b r_{ab}^{-1} \left((n_{ab}^i n_{ab}^j - \frac{1}{3}\delta^{ij} \right) \right\rangle \,. \tag{18}$$

Note that $(c^{-2} - 1)$ corresponds to the parameter δ plotted in Figure 2.

The electrodynamics given by Equation 15 can also be quantized, so that we may treat the interaction of photons with atoms via perturbation theory. The energy of a photon is $\hbar$ times its frequency ω, while its momentum is $\hbar\omega/c$. Using this approach, one finds that the difference in round trip travel times of light along the two arms of the interferometer in the Michelson-Morley experiment is given by $L_0(v^2/c)(c^{-2} - 1)$. The experimental null result then leads to the bound on $(c^{-2} - 1)$ shown on Figure 2. Similarly the anisotropy in energy levels is clearly illustrated by the tensorial terms in Equations 16 and 18; by evaluating $\tilde{E}_B^{ESij}$ for each nucleus in the various Hughes-Drever-type experiments and comparing with the experimental limits on energy differences, one obtains the extremely tight bounds also shown on Figure 2.

The behavior of moving atomic clocks can also be analysed in detail, and bounds on $(c^{-2} - 1)$ can be placed using results from tests of time dilation and of the propagation of light. In some cases, it is advantageous to combine the c^2 framework with a "kinematical" viewpoint that treats a general class of boost transformations between moving frames. Such kinematical approaches have been discussed by Robertson, Mansouri and Sexl, and Will (see Ref. 14).

For example, in the "JPL" experiment, in which the phases of two hydrogen masers connected by a fiberoptic link were compared as a function of the Earth's orientation, the predicted phase difference as a function of direction is, to first order in $\mathbf{V}$, the velocity of the Earth through the cosmic background,

$$\Delta\phi/\tilde{\phi} \approx -\frac{4}{3}(1 - c^2)(\mathbf{V}\cdot\mathbf{n} \;-\; \mathbf{V}\cdot\mathbf{n}_0) \,, \tag{19}$$

where $\tilde{\phi} = 2\pi\nu L$, ν is the maser frequency, $L = 21$ km is the baseline, and where $\mathbf{n}$ and $\mathbf{n}_0$ are unit vectors along the direction of propagation of the light, at a given time, and at the initial time of the experiment, respectively. The observed limit on a diurnal variation in the relative phase resulted in the bound $|c^{-2} - 1| < 3 \times 10^{-4}$. Tighter bounds were obtained from a "two-photon absorption" (TPA) experiment, and a 1960s series of "Mössbauer-rotor" experiments, which tested the isotropy of time dilation between a gamma ray emitter on the rim of a rotating disk and an absorber placed at the center.[14]

2.3 EEP, Particle Physics, and the Search for New Interactions

In 1986, as a result of a detailed reanalysis of Eötvös' original data, Fischbach *et al.* suggested the existence of a fifth force of nature, with a strength of about a percent that of gravity, but with a range (as defined by the range λ of a Yukawa potential, $e^{-r/\lambda}/r$) of a few hundred meters. This proposal dovetailed with earlier hints of a deviation from the inverse-square law of Newtonian gravitation derived from measurements of the gravity profile down deep mines in Australia, and with ideas from particle physics suggesting the possible presence of very low-mass particles with gravitational-strength couplings. During the next four years numerous experiments looked for evidence of the fifth force by searching for composition-dependent differences in acceleration, with variants of the Eötvös experiment or with free-fall Galileo-type experiments. Although two early experiments reported positive evidence, the others all yielded null results. Over the range between one and 10^4 meters, the null experiments produced upper limits on the strength of a postulated fifth force between 10^{-3} and 10^{-6} of the strength of gravity. Interpreted as tests of WEP (corresponding to the limit of infinite-range forces), the results of the free-fall Galileo experiment, and of the Eöt-Wash III experiment are shown in Figure 1. At the same time, tests of the inverse-square law of gravity were carried out by comparing variations in gravity measurements up tall towers or down mines or boreholes with gravity variations predicted using the inverse square law together with Earth models and surface gravity data mathematically "continued" up the tower or down the hole. Despite early reports of anomalies, independent tower, borehole and seawater measurements now show no evidence of a deviation. The consensus at present is that there is no credible experimen-

tal evidence for a fifth force of nature. For reviews and bibliographies, see Refs. 8,15,16 and 17.

Nevertheless, theoretical evidence continues to mount that EEP is *likely* to be violated at some level, whether by quantum gravity effects, by effects arising from string theory, or by hitherto undetected interactions, albeit at levels below those that motivated the fifth-force searches. Roughly speaking, in addition to the pure Einsteinian gravitational interaction, which respects EEP, theories such as string theory predict other interactions which do not. In string theory, for example, the existence of such EEP-violating fields is assured, but the theory is not yet mature enough to enable calculation of their strength (relative to gravity), or their range (whether they are long range, like gravity, or short range, like the nuclear and weak interactions, or too short-range to be detectable) (for further discussion see Ref. 6).

In one simple example, one can write the Lagrangian for the low-energy limit of string theory in the so-called "Einstein frame", in which the gravitational Lagrangian is purely general relativistic:

$$\begin{aligned}\tilde{\mathcal{L}} = \quad & \sqrt{-\tilde{g}}\Big(\tilde{g}^{\mu\nu}\Big[\tfrac{1}{2\kappa}\tilde{R}_{\mu\nu} - \tfrac{1}{2}\tilde{G}(\varphi)\partial_\mu\varphi\partial_\nu\varphi\Big] - U(\varphi)\tilde{g}^{\mu\nu}\tilde{g}^{\alpha\beta}F_{\mu\alpha}F_{\nu\beta} \\ & + \bar{\tilde{\psi}}\Big[i\tilde{e}^\mu_a\gamma^a(\partial_\mu + \tilde{\Omega}_\mu + qA_\mu) - \tilde{M}(\varphi)\Big]\tilde{\psi}\Big)\,, \end{aligned} \tag{20}$$

where $\tilde{g}_{\mu\nu}$ is the non-physical metric, $\tilde{R}_{\mu\nu}$ is the Ricci tensor derived from it, φ is a dilaton field, and $\tilde{G}$, U and $\tilde{M}$ are functions of φ. The Lagrangian includes that for the electromagnetic field $F_{\mu\nu}$, and that for particles, written in terms of Dirac spinors $\tilde{\psi}$. This is not a metric representation because of the coupling of φ to matter via $\tilde{M}(\varphi)$ and $U(\varphi)$. A conformal transformation $\tilde{g}_{\mu\nu} = F(\varphi)g_{\mu\nu}$, $\tilde{\psi} = F(\varphi)^{-3/4}\psi$, puts the Lagrangian in the form ("Jordan" frame)

$$\begin{aligned}\mathcal{L} = \quad & \sqrt{-g}\Big(g^{\mu\nu}\Big[\tfrac{1}{2\kappa}F(\varphi)R_{\mu\nu} - \tfrac{1}{2}F(\varphi)\tilde{G}(\varphi)\partial_\mu\varphi\partial_\nu\varphi + \tfrac{3}{4\kappa F(\varphi)}\partial_\mu F\partial_\nu F\Big] \\ & - U(\varphi)g^{\mu\nu}g^{\alpha\beta}F_{\mu\alpha}F_{\nu\beta} + \bar{\psi}\Big[ie^\mu_a\gamma^a(\partial_\mu + \Omega_\mu + qA_\mu) - \tilde{M}(\varphi)F^{1/2}\Big]\psi\Big)\,. \end{aligned} \tag{21}$$

One may choose $F(\varphi) = \text{const}/\tilde{M}(\varphi)^2$ so that the particle Lagrangian takes the metric form (no coupling to φ), but the electromagnetic Lagrangian will still couple non-metrically to $U(\varphi)$. The gravitational Lagrangian here takes the form of a scalar-tensor theory (Sec. 3.3.2). But the non-metric electromagnetic term will, in general, produce violations of EEP.

Thus, EEP and related tests are now viewed as ways to discover or place constraints on new physical interactions, or as a branch of "non-accelerator particle physics", searching for the possible imprints of high-energy particle effects in the low-energy realm of gravity. Whether current or proposed experiments can actually probe these phenomena meaningfully is an open question at the moment, largely because of a dearth of firm theoretical predictions. Despite this uncertainty, a number of experimental possibilities are being explored.

The concept of an equivalence principle experiment in space has been developed, with the potential to test WEP to 10^{-18}. Known generically as Satellite Test of the Equivalence Principle (STEP), various versions of the project are under consideration as possible joint efforts of NASA and the European Space Agency (ESA). The gravitational redshift could be improved to the 10^{-10} level using atomic clocks on board a spacecraft which would travel to within four solar radii of the Sun. Laboratory tests of the gravitational inverse square law at sub-millimeter scales are being developed as ways to search for new short-range interactions; the challenge of these experiments is to distinguish gravitation-like interactions from electromagnetic and quantum mechanical (Casimir) effects.

3 Tests of Post-Newtonian Gravity

3.1 Metric Theories of Gravity and the Strong Equivalence Principle

3.1.1 Universal Coupling and the Metric Postulates

The overwhelming empirical evidence supporting the Einstein equivalence principle, discussed in the previous section, supports the conclusion that the only theories of gravity that have a hope of being viable are metric theories, or possibly theories that are metric apart from possible weak or short-range non-metric couplings (as in string theory). Therefore for the remainder of these lectures, we shall turn our attention exclusively to metric theories of gravity, which assume that (i) there exists a symmetric metric, (ii) test bodies follow geodesics of the metric, and (iii) in local Lorentz frames, the non-gravitational laws of physics are those of special relativity.

The property that all non-gravitational fields should couple in the same manner

to a single gravitational field is sometimes called "universal coupling". Because of it, one can discuss the metric as a property of spacetime itself rather than as a field over spacetime. This is because its properties may be measured and studied using a variety of different experimental devices, composed of different non-gravitational fields and particles, and, because of universal coupling, the results will be independent of the device. Thus, for instance, the proper time between two events is a characteristic of spacetime and of the location of the events, not of the clocks used to measure it.

Consequently, if EEP is valid, the non-gravitational laws of physics may be formulated by taking their special relativistic forms in terms of the Minkowski metric $\boldsymbol{\eta}$ and simply "going over" to new forms in terms of the curved spacetime metric $\mathbf{g}$, using the mathematics of differential geometry. The details of this "going over" can be found in standard textbooks (Refs. 18,19; TEGP 3.2)

3.1.2 The Strong Equivalence Principle

In any metric theory of gravity, matter and non-gravitational fields respond only to the spacetime metric $\mathbf{g}$. In principle, however, there could exist other gravitational fields besides the metric, such as scalar fields, vector fields, and so on. If, by our strict definition of metric theory, matter does not couple to these fields what can their role in gravitation theory be? Their role must be that of mediating the manner in which matter and non-gravitational fields generate gravitational fields and produce the metric; once determined, however, the metric alone acts back on the matter in the manner prescribed by EEP.

What distinguishes one metric theory from another, therefore, is the number and kind of gravitational fields it contains in addition to the metric, and the equations that determine the structure and evolution of these fields. From this viewpoint, one can divide all metric theories of gravity into two fundamental classes: "purely dynamical" and "prior-geometric".

By "purely dynamical metric theory" we mean any metric theory whose gravitational fields have their structure and evolution determined by coupled partial differential field equations. In other words, the behavior of each field is influenced to some extent by a coupling to at least one of the other fields in the theory. By "prior geometric" theory, we mean any metric theory that contains "absolute elements", fields or equations whose structure and evolution are given

a priori, and are independent of the structure and evolution of the other fields of the theory. These "absolute elements" typically include flat background metrics $\boldsymbol{\eta}$, cosmic time coordinates t, algebraic relationships among otherwise dynamical fields, such as $g_{\mu\nu} = h_{\mu\nu} + k_\mu k_\nu$, where $h_{\mu\nu}$ and k_μ may be dynamical fields.

General relativity is a purely dynamical theory since it contains only one gravitational field, the metric itself, and its structure and evolution are governed by partial differential equations (Einstein's equations). Brans-Dicke theory and its generalizations are purely dynamical theories; the field equation for the metric involves the scalar field (as well as the matter as source), and that for the scalar field involves the metric. Rosen's bimetric theory is a prior-geometric theory: it has a non-dynamical, Riemann-flat background metric, $\boldsymbol{\eta}$, and the field equations for the physical metric $\mathbf{g}$ involve $\boldsymbol{\eta}$.

By discussing metric theories of gravity from this broad point of view, it is possible to draw some general conclusions about the nature of gravity in different metric theories, conclusions that are reminiscent of the Einstein equivalence principle, but that are subsumed under the name "strong equivalence principle".

Consider a local, freely falling frame in any metric theory of gravity. Let this frame be small enough that inhomogeneities in the external gravitational fields can be neglected throughout its volume. On the other hand, let the frame be large enough to encompass a system of gravitating matter and its associated gravitational fields. The system could be a star, a black hole, the solar system or a Cavendish experiment. Call this frame a "quasi-local Lorentz frame" . To determine the behavior of the system we must calculate the metric. The computation proceeds in two stages. First we determine the external behavior of the metric and gravitational fields, thereby establishing boundary values for the fields generated by the local system, at a boundary of the quasi-local frame "far" from the local system. Second, we solve for the fields generated by the local system. But because the metric is coupled directly or indirectly to the other fields of the theory, its structure and evolution will be influenced by those fields, and in particular by the boundary values taken on by those fields far from the local system. This will be true even if we work in a coordinate system in which the asymptotic form of $g_{\mu\nu}$ in the boundary region between the local system and the external world is that of the Minkowski metric. Thus the gravitational environment in which the local gravitating system resides can influence the metric generated by the local system via the boundary values of the auxiliary fields. Consequently, the results of local

gravitational experiments may depend on the location and velocity of the frame relative to the external environment. Of course, local *non*-gravitational experiments are unaffected since the gravitational fields they generate are assumed to be negligible, and since those experiments couple only to the metric, whose form can always be made locally Minkowskian at a given spacetime event. Local gravitational experiments might include Cavendish experiments, measurement of the acceleration of massive self-gravitating bodies, studies of the structure of stars and planets, or analyses of the periods of "gravitational clocks". We can now make several statements about different kinds of metric theories.

(i) A theory which contains only the metric $\mathbf{g}$ yields local gravitational physics which is independent of the location and velocity of the local system. This follows from the fact that the only field coupling the local system to the environment is $\mathbf{g}$, and it is always possible to find a coordinate system in which $\mathbf{g}$ takes the Minkowski form at the boundary between the local system and the external environment. Thus the asymptotic values of $g_{\mu\nu}$ are constants independent of location, and are asymptotically Lorentz invariant, thus independent of velocity. General relativity is an example of such a theory.

(ii) A theory which contains the metric $\mathbf{g}$ and dynamical scalar fields φ_A yields local gravitational physics which may depend on the location of the frame but which is independent of the velocity of the frame. This follows from the asymptotic Lorentz invariance of the Minkowski metric and of the scalar fields, but now the asymptotic values of the scalar fields may depend on the location of the frame. An example is Brans-Dicke theory, where the asymptotic scalar field determines the effective value of the gravitational constant, which can thus vary as φ varies.

(iii) A theory which contains the metric $\mathbf{g}$ and additional dynamical vector or tensor fields or prior-geometric fields yields local gravitational physics which may have both location and velocity-dependent effects.

These ideas can be summarized in the strong equivalence principle (SEP), which states that (i) WEP is valid for self-gravitating bodies as well as for test bodies, (ii) the outcome of any local test experiment is independent of the velocity of the (freely falling) apparatus, and (iii) the outcome of any local test experiment is independent of where and when in the universe it is performed. The distinction between SEP and EEP is the inclusion of bodies with self-gravitational interactions (planets, stars) and of experiments involving gravitational forces (Cavendish experiments, gravimeter measurements). Note that SEP contains EEP as the spe-

cial case in which local gravitational forces are ignored.

The above discussion of the coupling of auxiliary fields to local gravitating systems indicates that if SEP is strictly valid, there must be one and only one gravitational field in the universe, the metric $\mathbf{g}$. These arguments are only suggestive however, and no rigorous proof of this statement is available at present. Empirically it has been found that every metric theory other than GR introduces auxiliary gravitational fields, either dynamical or prior geometric, and thus predicts violations of SEP at some level (here we ignore quantum-theory inspired modifications to GR involving "R^2" terms). General relativity seems to be the only metric theory that embodies SEP completely. This lends some credence to the conjecture SEP $\rightarrow$ General Relativity. In Sec. 3.6, we shall discuss experimental evidence for the validity of SEP.

3.2 The Parametrized Post-Newtonian Formalism

Despite the possible existence of long-range gravitational fields in addition to the metric in various metric theories of gravity, the postulates of those theories demand that matter and non-gravitational fields be completely oblivious to them. The only gravitational field that enters the equations of motion is the metric $\mathbf{g}$. The role of the other fields that a theory may contain can only be that of helping to generate the spacetime curvature associated with the metric. Matter may create these fields, and they plus the matter may generate the metric, but they cannot act back directly on the matter. Matter responds only to the metric.

Thus the metric and the equations of motion for matter become the primary entities for calculating observable effects, and all that distinguishes one metric theory from another is the particular way in which matter and possibly other gravitational fields generate the metric.

The comparison of metric theories of gravity with each other and with experiment becomes particularly simple when one takes the slow-motion, weak-field limit. This approximation, known as the post-Newtonian limit, is sufficiently accurate to encompass most solar-system tests that can be performed in the foreseeable future. It turns out that, in this limit, the spacetime metric $\mathbf{g}$ predicted by nearly every metric theory of gravity has the same structure. It can be written as an expansion about the Minkowski metric ($\eta_{\mu\nu} = \mathrm{diag}(-1, 1, 1, 1)$) in terms of dimensionless gravitational potentials of varying degrees of smallness. These

Parameter	What it measures relative to GR	Value in GR	Value in semi-conservative theories	Value in fully-conservative theories
γ	How much space-curvature produced by unit rest mass?	1	γ	γ
β	How much "nonlinearity" in the superposition law for gravity?	1	β	β
ξ	Preferred-location effects?	0	ξ	ξ
α_1	Preferred-frame effects?	0	α_1	0
α_2		0	α_2	0
α_3		0	0	0
α_3	Violation of conservation	0	0	0
ζ_1	of total momentum?	0	0	0
ζ_2		0	0	0
ζ_3		0	0	0
ζ_4		0	0	0

Table 2. The PPN Parameters and their significance (note that α_3 has been shown twice to indicate that it is a measure of two effects)

potentials are constructed from the matter variables (Box 2) in imitation of the Newtonian gravitational potential

$$U(\mathbf{x},t) \equiv \int \rho(\mathbf{x}',t)|\mathbf{x}-\mathbf{x}'|^{-1}d^3x' \,. \tag{22}$$

The "order of smallness" is determined according to the rules $U \sim v^2 \sim \Pi \sim p/\rho \sim O(2)$, $v^i \sim |d/dt|/|d/dx| \sim 0(1)$, and so on.

A consistent post-Newtonian limit requires determination of g_{00} correct through O(4), g_{0i} through O(3) and g_{ij} through O(2) (for details see TEGP 4.1). The only way that one metric theory differs from another is in the numerical values of the coefficients that appear in front of the metric potentials. The parametrized post-Newtonian (PPN) formalism inserts parameters in place of these coefficients,

parameters whose values depend on the theory under study. In the current version of the PPN formalism, summarized in Box 2, ten parameters are used, chosen in such a manner that they measure or indicate general properties of metric theories of gravity (Table 2). The parameters γ and β are the usual Eddington-Robertson-Schiff parameters used to describe the "classical" tests of GR; ξ is non-zero in any theory of gravity that predicts preferred-location effects such as a galaxy-induced anisotropy in the local gravitational constant G_L (also called "Whitehead" effects); α_1, α_2, α_3 measure whether or not the theory predicts post-Newtonian preferred-frame effects; α_3, ζ_1, ζ_2, ζ_3, ζ_4 measure whether or not the theory predicts violations of global conservation laws for total momentum. In Table 2 we show the values these parameters take (i) in GR, (ii) in any theory of gravity that possesses conservation laws for total momentum, called "semi-conservative" (any theory that is based on an invariant action principle is semi-conservative, and (iii) in any theory that in addition possesses six global conservation laws for angular momentum, called "fully conservative" (such theories automatically predict no post-Newtonian preferred-frame effects). Semi-conservative theories have five free PPN parameters (γ, β, ξ, α_1, α_2) while fully conservative theories have three (γ, β , ξ).

The PPN formalism was pioneered by Kenneth Nordtvedt, who studied the post-Newtonian metric of a system of gravitating point masses, extending earlier work by Eddington, Robertson and Schiff (TEGP 4.2). A general and unified version of the PPN formalism was developed by Will and Nordtvedt. The canonical version, with conventions altered to be more in accord with standard textbooks such as MTW, is discussed in detail in TEGP, Chapter 4. Other versions of the PPN formalism have been developed to deal with point masses with charge, fluid with anisotropic stresses, bodies with strong internal gravity, and post-post-Newtonian effects (TEGP 4.2, 14.2).

3.3 Competing Theories of Gravity

One of the important applications of the PPN formalism is the comparison and classification of alternative metric theories of gravity. The population of viable theories has fluctuated over the years as new effects and tests have been discovered, largely through the use of the PPN framework, which eliminated many theories thought previously to be viable. The theory population has also fluctuated as

Box 2. The Parametrized Post-Newtonian Formalism

1. **Coordinate System:** The framework uses a nearly globally Lorentz coordinate system in which the coordinates are (t, x^1, x^2, x^3). Three-dimensional, Euclidean vector notation is used throughout. All coordinate arbitrariness ("gauge freedom") has been removed by specialization of the coordinates to the standard PPN gauge (TEGP 4.2). Units are chosen so that $G = c = 1$, where G is the physically measured Newtonian constant far from the solar system.

2. **Matter Variables:**

   - ρ = density of rest mass as measured in a local freely falling frame momentarily comoving with the gravitating matter.
   - $v^i = (dx^i/dt)$ = coordinate velocity of the matter.
   - w^i = coordinate velocity of PPN coordinate system relative to the mean rest-frame of the universe.
   - p = pressure as measured in a local freely falling frame momentarily comoving with the matter.
   - Π = internal energy per unit rest mass. It includes all forms of non-rest-mass, non-gravitational energy, *e.g.* energy of compression and thermal energy.

3. **PPN Parameters:**

   γ , β , ξ , α_1 , α_2 , α_3 , ζ_1 , ζ_2 , ζ_3 , ζ_4 .

4. **Metric:**

$$
\begin{aligned}
g_{00} &= -1 + 2U - 2\beta U^2 - 2\xi\Phi_W + (2\gamma + 2 + \alpha_3 + \zeta_1 - 2\xi)\Phi_1 \\
&\quad +2(3\gamma - 2\beta + 1 + \zeta_2 + \xi)\Phi_2 + 2(1 + \zeta_3)\Phi_3 + 2(3\gamma + 3\zeta_4 - 2\xi)\Phi_4 \\
&\quad -(\zeta_1 - 2\xi)\mathcal{A} - (\alpha_1 - \alpha_2 - \alpha_3)w^2 U - \alpha_2 w^i w^j U_{ij} + (2\alpha_3 - \alpha_1)w^i V_i \\
g_{0i} &= -\frac{1}{2}(4\gamma + 3 + \alpha_1 - \alpha_2 + \zeta_1 - 2\xi)V_i - \frac{1}{2}(1 + \alpha_2 - \zeta_1 + 2\xi)W_i \\
&\quad -\frac{1}{2}(\alpha_1 - 2\alpha_2)w^i U - \alpha_2 w^j U_{ij} \\
g_{ij} &= (1 + 2\gamma U)\delta_{ij}
\end{aligned}
$$

Box 2. (continued)

1. **Metric Potentials:**

$$
\begin{aligned}
U &= \int \frac{\rho'}{|\mathbf{x}-\mathbf{x}'|} d^3x' , \qquad U_{ij} = \int \frac{\rho'(x-x')_i (x-x')_j}{|\mathbf{x}-\mathbf{x}'|^3} d^3x' \\
\Phi_W &= \int \frac{\rho' \rho'' (\mathbf{x}-\mathbf{x}')}{|\mathbf{x}-\mathbf{x}'|^3} \cdot \left(\frac{\mathbf{x}'-\mathbf{x}''}{|\mathbf{x}-\mathbf{x}''|} - \frac{\mathbf{x}-\mathbf{x}''}{|\mathbf{x}'-\mathbf{x}''|} \right) d^3x' d^3x'' \\
\mathcal{A} &= \int \frac{\rho' [\mathbf{v}' \cdot (\mathbf{x}-\mathbf{x}')]^2}{|\mathbf{x}-\mathbf{x}'|^3} d^3x' , \qquad \Phi_1 = \int \frac{\rho' v'^2}{|\mathbf{x}-\mathbf{x}'|} d^3x' \\
\Phi_2 &= \int \frac{\rho' U'}{|\mathbf{x}-\mathbf{x}'|} d^3x' , \quad \Phi_3 = \int \frac{\rho' \Pi'}{|\mathbf{x}-\mathbf{x}'|} d^3x' , \quad \Phi_4 = \int \frac{p'}{|\mathbf{x}-\mathbf{x}'|} d^3x' \\
V_i &= \int \frac{\rho' v'_i}{|\mathbf{x}-\mathbf{x}'|} d^3x' , \qquad W_i = \int \frac{\rho' [\mathbf{v}' \cdot (\mathbf{x}-\mathbf{x}')](x-x')_i}{|\mathbf{x}-\mathbf{x}'|^3} d^3x'
\end{aligned}
$$

2. **Stress-Energy Tensor** (perfect fluid)

$$
\begin{aligned}
T^{00} &= \rho(1 + \Pi + v^2 + 2U) \\
T^{0i} &= \rho v^i (1 + \Pi + v^2 + 2U + p/\rho) \\
T^{ij} &= \rho v^i v^j (1 + \Pi + v^2 + 2U + p/\rho) + p\delta^{ij}(1 - 2\gamma U)
\end{aligned}
$$

3. **Equations of Motion**

- Stressed Matter, $\quad T^{\mu\nu}{}_{;\nu} = 0$
- Test Bodies, $\quad d^2x^\mu/d\lambda^2 + \Gamma^\mu{}_{\nu\lambda}(dx^\nu/d\lambda)(dx^\lambda/d\lambda) = 0$
- Maxwell's Equations, $\quad F^{\mu\nu}{}_{;\nu} = 4\pi J^\mu \qquad F_{\mu\nu} = A_{\nu;\mu} - A_{\mu;\nu}$

new, potentially viable theories have been invented.

In these lectures, we shall focus on general relativity and the general class of scalar-tensor modifications of it, of which the Jordan-Fierz-Brans-Dicke theory (Brans-Dicke, for short) is the classic example. The reasons are several-fold:

- A full compendium of alternative theories is given in TEGP, Chapter 5.
- Many alternative metric theories developed during the 1970s and 1980s could be viewed as "straw-man" theories, invented to prove that such theories exist or to illustrate particular properties. Few of these could be regarded as well-motivated theories from the point of view, say, of field theory or particle physics. Examples are the vector-tensor theories studied by Will, Nordtvedt and Hellings.
- A number of theories fall into the class of "prior-geometric" theories, with absolute elements such as a flat background metric in addition to the physical metric. Most of these theories predict "preferred-frame" effects, that have been tightly constrained by observations (see Sec. 3.6.2). An example is Rosen's bimetric theory.
- A large number of alternative theories of gravity predict gravitational-wave emission substantially different from that of general relativity, in strong disagreement with observations of the binary pulsar (see Sec. 4).
- Scalar-tensor modifications of GR have recently become very popular in cosmological model building and in unification schemes, such as string theory.

3.3.1 General Relativity

The metric $\mathbf{g}$ is the sole dynamical field and the theory contains no arbitrary functions or parameters, apart from the value of the Newtonian coupling constant G, which is measurable in laboratory experiments. Throughout these lectures, we ignore the cosmological constant λ. Although λ has significance for quantum field theory, quantum gravity, and cosmology, on the scale of the solar-system or of stellar systems, its effects are negligible, for values of λ corresponding to a cosmological closure density.

The field equations of GR are derivable from an invariant action principle $\delta I = 0$, where

$$I = (16\pi G)^{-1} \int R(-g)^{1/2} d^4x + I_m(\psi_m, g_{\mu\nu}) \,, \tag{23}$$

Theory	Arbitrary Functions or Constants	Cosmic Matching Parameters	PPN Parameters				
			γ	β	ξ	α_1	α_2
General Relativity	none	none	1	1	0	0	0
Scalar-Tensor							
Brans-Dicke	ω	ϕ_0	$\frac{(1+\omega)}{(2+\omega)}$	1	0	0	0
General	$A(\varphi)$, $V(\varphi)$	φ_0	$\frac{(1+\omega)}{(2+\omega)}$	$1+\Lambda$	0	0	0
Rosen's Bimetric	none	c_0, c_1	1	1	0	0	$\frac{c_0}{c_1}-1$

Table 3. Metric Theories and Their PPN Parameter Values ($\alpha_3 = \zeta_i = 0$ for all cases)

where R is the Ricci scalar, and I_m is the matter action, which depends on matter fields ψ_m universally coupled to the metric $\mathbf{g}$. By varying the action with respect to $g_{\mu\nu}$, we obtain the field equations

$$G_{\mu\nu} \equiv R_{\mu\nu} - \frac{1}{2} g_{\mu\nu} R = 8\pi G T_{\mu\nu} \,, \tag{24}$$

where $T_{\mu\nu}$ is the matter energy-momentum tensor. General covariance of the matter action implies the equations of motion ${T^{\mu\nu}}_{;\nu} = 0$; varying I_m with respect to ψ_M yields the matter field equations. By virtue of the *absence* of prior-geometric elements, the equations of motion are also a consequence of the field equations via the Bianchi identities ${G^{\mu\nu}}_{;\nu} = 0$.

The general procedure for deriving the post-Newtonian limit is spelled out in TEGP 5.1, and is described in detail for GR in TEGP 5.2. The PPN parameter values are listed in Table 3.

3.3.2 Scalar-Tensor Theories

These theories contain the metric $\mathbf{g}$, a scalar field φ, a potential function $V(\varphi)$, and a coupling function $A(\varphi)$ (generalizations to more than one scalar field have also been carried out[20]). For some purposes, the action is conveniently written in a non-metric representation, sometimes denoted the "Einstein frame", in which

the gravitational action looks exactly like that of GR:

$$\tilde{I} = (16\pi G)^{-1} \int [\tilde{R} - 2\tilde{g}^{\mu\nu}\partial_\mu\varphi\partial_\nu\varphi - V(\varphi)](-\tilde{g})^{1/2} d^4x + I_m(\psi_m, A^2(\varphi)\tilde{g}_{\mu\nu}) \,, \quad (25)$$

where $\tilde{R} \equiv \tilde{g}^{\mu\nu}\tilde{R}_{\mu\nu}$ is the Ricci scalar of the "Einstein" metric $\tilde{g}_{\mu\nu}$. (Apart from the scalar potential term $V(\varphi)$, this corresponds to Equation (20) with $\tilde{G}(\varphi) \equiv (4\pi G)^{-1}$, $U(\varphi) \equiv 1$, and $\tilde{M}(\varphi) \propto A(\varphi)$.) This representation is a "non-metric" one because the matter fields ψ_m couple to a combination of φ and $\tilde{g}_{\mu\nu}$. Despite appearances, however, it is a metric theory, because it can be put into a metric representation by identifying the "physical metric"

$$g_{\mu\nu} \equiv A^2(\varphi)\tilde{g}_{\mu\nu} \,. \quad (26)$$

The action can then be rewritten in the metric form

$$I = (16\pi G)^{-1} \int [\phi R - \phi^{-1}\omega(\phi) g^{\mu\nu}\partial_\mu\phi\partial_\nu\phi - \phi^2 V](-g)^{1/2} d^4x + I_m(\psi_m, g_{\mu\nu}) \,, \quad (27)$$

where

$$\begin{aligned} \phi &\equiv A(\varphi)^{-2} \,, \\ 3 + 2\omega(\phi) &\equiv \alpha(\varphi)^{-2} \,, \\ \alpha(\varphi) &\equiv d(\ln A(\varphi))/d\varphi \,. \end{aligned} \quad (28)$$

The Einstein frame is useful for discussing general characteristics of such theories, and for some cosmological applications, while the metric representation is most useful for calculating observable effects. The field equations, post-Newtonian limit and PPN parameters are discussed in TEGP 5.3, and the values of the PPN parameters are listed in Table 3.

The parameters that enter the post-Newtonian limit are

$$\omega \equiv \omega(\phi_0) \qquad \Lambda \equiv [(d\omega/d\phi)(3 + 2\omega)^{-2}(4 + 2\omega)^{-1}]_{\phi_0} \,, \quad (29)$$

where ϕ_0 is the value of ϕ today far from the system being studied, as determined by appropriate cosmological boundary conditions. The following formula is also useful: $1/(2 + \omega) = 2\alpha_0^2/(1 + \alpha_0^2)$. In Brans-Dicke theory ($\omega(\phi) =$ constant), the larger the value of ω, the smaller the effects of the scalar field, and in the limit $\omega \to \infty$ ($\alpha_0 \to 0$), the theory becomes indistinguishable from GR in all its predictions. In more general theories, the function $\omega(\phi)$ could have the property

that, at the present epoch, and in weak-field situations, the value of the scalar field ϕ_0 is such that, ω is very large and Λ is very small (theory almost identical to GR today), but that for past or future values of ϕ, or in strong-field regions such as the interiors of neutron stars, ω and Λ could take on values that would lead to significant differences from GR. Indeed, Damour and Nordtvedt have shown that in such general scalar-tensor theories, GR is a natural "attractor": regardless of how different the theory may be from GR in the early universe (apart from special cases), cosmological evolution naturally drives the fields toward small values of the function α, thence to large ω. Estimates of the expected relic deviations from GR today in such theories depend on the cosmological model, but range from 10^{-5} to a few times 10^{-7} for $1-\gamma$ (Ref. 21).

Scalar fields coupled to gravity or matter are also ubiquitous in particle-physics-inspired models of unification, such as string theory. In some models, the coupling to matter may lead to violations of WEP, which are tested by Eötvös-type experiments. In many models the scalar field is massive; if the Compton wavelength is of macroscopic scale, its effects are those of a "fifth force". Only if the theory can be cast as a metric theory with a scalar field of infinite range or of range long compared to the scale of the system in question (solar system) can the PPN framework be strictly applied. If the mass of the scalar field is sufficiently large that its range is microscopic, then, on solar-system scales, the scalar field is suppressed, and the theory is essentially equivalent to general relativity. This is the case, for example in the "oscillating-G" models of Accetta, Steinhardt and Will (see Ref. 22), in which the potential function $V(\varphi)$ contains both quadratic (mass) and quartic (self-interaction) terms, causing the scalar field to oscillate (the initial amplitude of oscillation is provided by an inflationary epoch); high-frequency oscillations in the "effective" Newtonian constant $G_{eff} \equiv G/\phi = GA(\varphi)^2$ then result. The energy density in the oscillating scalar field can be enough to provide a cosmological closure density without resorting to dark matter, yet the value of ω today is so large that the theory's local predictions are experimentally indistinguishable from GR. In other models, explored by Damour and Esposito-Farèse,[23] non-linear scalar-field couplings can lead to "spontaneous scalarization" inside strong-field objects such as neutron stars, leading to large deviations from GR, even in the limit of very large ω.

3.4 Tests of the Parameter γ

With the PPN formalism in hand, we are now ready to confront gravitation theories with the results of solar-system experiments. In this section we focus on tests of the parameter γ, consisting of the deflection of light and the time delay of light.

3.4.1 The Deflection of Light

A light ray (or photon) which passes the Sun at a distance d is deflected by an angle

$$\delta\theta = \frac{1}{2}(1+\gamma)(4m_\odot/d)[(1+\cos\Phi)/2] \tag{30}$$

(TEGP 7.1), where $m_\odot$ is the mass of the Sun and Φ is the angle between the Earth-Sun line and the incoming direction of the photon (Figure 4). For a grazing ray, $d \approx d_\odot$, $\Phi \approx 0$, and

$$\delta\theta \;\approx\; \frac{1}{2}(1+\gamma)1.''75\,, \tag{31}$$

independent of the frequency of light. Another, more useful expression gives the change in the relative angular separation between an observed source of light and a nearby reference source as both rays pass near the Sun:

$$\delta\theta = \frac{1}{2}(1+\gamma)\left[-\frac{4m_\odot}{d}\cos\chi + \frac{4m_\odot}{d_r}\left(\frac{1+\cos\Phi_r}{2}\right)\right]\,, \tag{32}$$

where d and d_r are the distances of closest approach of the source and reference rays respectively, Φ_r is the angular separation between the Sun and the reference source, and χ is the angle between the Sun-source and the Sun-reference directions, projected on the plane of the sky (Figure 4). Thus, for example, the relative angular separation between the two sources may vary if the line of sight of one of them passes near the Sun ($d \sim R_\odot$, $d_r \gg d$, χ varying with time).

It is interesting to note that the classic derivations of the deflection of light that use only the principle of equivalence or the corpuscular theory of light yield only the "1/2" part of the coefficient in front of the expression in Equation 30. But the result of these calculations is the deflection of light relative to local straight lines, as defined for example by rigid rods; however, because of space curvature around the Sun, determined by the PPN parameter γ, local straight lines are bent relative to asymptotic straight lines far from the Sun by just enough to yield the remaining factor "$\gamma/2$". The first factor "1/2" holds in any metric theory, the

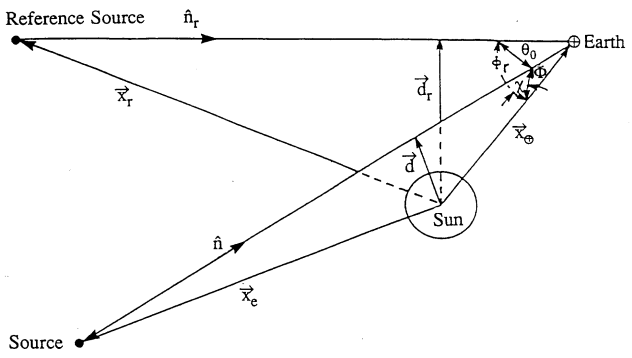

Fig. 4. Geometry of light deflection measurements.

second "$\gamma/2$" varies from theory to theory. Thus, calculations that purport to derive the full deflection using the equivalence principle alone are incorrect.

The prediction of the full bending of light by the Sun was one of the great successes of Einstein's GR. Eddington's confirmation of the bending of optical starlight observed during a solar eclipse in the first days following World War I helped make Einstein famous. However, the experiments of Eddington and his co-workers had only 30 percent accuracy, and succeeding experiments were not much better: the results were scattered between one half and twice the Einstein value (Figure 5), and the accuracies were low.

However, the development of very-long-baseline radio interferometry (VLBI) produced greatly improved determinations of the deflection of light. These techniques now have the capability of measuring angular separations and changes in angles as small as 100 microarcseconds. Early measurements took advantage of a series of heavenly coincidences: each year, groups of strong quasistellar radio sources pass very close to the Sun (as seen from the Earth), including the group 3C273, 3C279, and 3C48, and the group 0111+02, 0119+11 and 0116+08. As the Earth moves in its orbit, changing the lines of sight of the quasars relative to the Sun, the angular separation $\delta\theta$ between pairs of quasars varies (Equation 32). The time variation in the quantities d, d_r, χ and Φ_r in Equation 32 is determined using an accurate ephemeris for the Earth and initial directions for the quasars, and the resulting prediction for $\delta\theta$ as a function of time is used as a basis for a least-squares fit of the measured $\delta\theta$, with one of the fitted parameters being the coefficient $\frac{1}{2}(1+\gamma)$. A number of measurements of this kind over the period

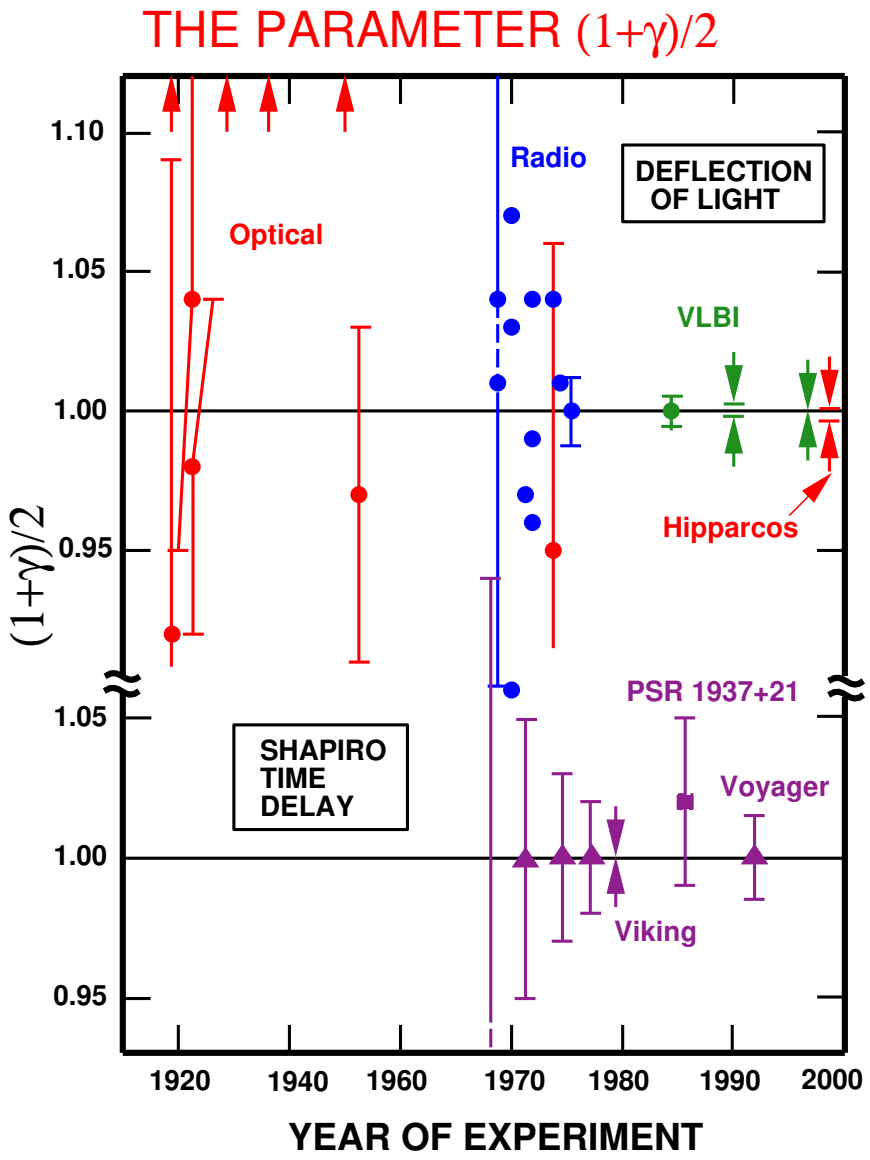

Fig. 5. Measurements of the coefficient $(1+\gamma)/2$ from light deflection and time delay measurements. General relativity value is unity. Arrows denote anomalously large values from 1929 and 1936 eclipse expeditions. Shapiro time-delay measurements using Viking spacecraft and VLBI light deflection measurements yielded agreement with GR to 0.1 percent. Hipparcos denotes the optical astrometry satellite.

1969–1975 yielded an accurate determination of the coefficient $\frac{1}{2}(1+\gamma)$ which has the value unity in GR. Their results are shown in Figure 5.

A recent series of transcontinental and intercontinental VLBI quasar and radio galaxy observations made primarily to monitor the Earth's rotation ("VLBI " in Figure 5) was sensitive to the deflection of light over almost the entire celestial sphere (at 90° from the Sun, the deflection is still 4 milliarcseconds). A recent analysis of VLBI data yielded $(1+\gamma)/2 = 0.99997 \pm 0.00016$.[24] Analysis of observations made by the Hipparcos optical astrometry satellite yielded a test at the level of 0.3 percent.[25] A VLBI measurement of the deflection of light by Jupiter was reported; the predicted deflection of about 300 microarcseconds was seen with about 50 percent accuracy.

3.4.2 The Time Delay of Light

A radar signal sent across the solar system past the Sun to a planet or satellite and returned to the Earth suffers an additional non-Newtonian delay in its round-trip travel time, given by (see Figure 4)

$$\delta t = 2(1+\gamma) m_\odot \ln[(r_\oplus \; + \; \mathbf{x}_\oplus \cdot \mathbf{n})(r_e - \mathbf{x}_e \cdot \mathbf{n})/d^2] \tag{33}$$

(TEGP 7.2). For a ray which passes close to the Sun,

$$\delta t \approx \frac{1}{2}(1+\gamma)[240 - 20\ln(d^2/r)]\ \mu\mathrm{s}\,, \tag{34}$$

where d is the distance of closest approach of the ray in solar radii, and r is the distance of the planet or satellite from the Sun, in astronomical units.

In the two decades following Irwin Shapiro's 1964 discovery of this effect as a theoretical consequence of general relativity, several high-precision measurements were made using radar ranging to targets passing through superior conjunction. Since one does not have access to a "Newtonian" signal against which to compare the round-trip travel time of the observed signal, it is necessary to do a differential measurement of the variations in round-trip travel times as the target passes through superior conjunction, and to look for the logarithmic behavior of Equation 34. In order to do this accurately however, one must take into account the variations in round-trip travel time due to the orbital motion of the target relative to the Earth. This is done by using radar-ranging (and possibly other) data on the target taken when it is far from superior conjunction (*i.e.*, when the

time-delay term is negligible) to determine an accurate ephemeris for the target, using the ephemeris to predict the PPN coordinate trajectory $\mathbf{x}_e(t)$ near superior conjunction, then combining that trajectory with the trajectory of the Earth $\mathbf{x}_\oplus(t)$ to determine the Newtonian round-trip time and the logarithmic term in Equation 34. The resulting predicted round-trip travel times in terms of the unknown coefficient $\frac{1}{2}(1+\gamma)$ are then fit to the measured travel times using the method of least-squares, and an estimate obtained for $\frac{1}{2}(1+\gamma)$.

The targets employed included planets, such as Mercury or Venus, used as a passive reflectors of the radar signals ("passive radar"), and artificial satellites, such as Mariners 6 and 7, and Voyager 2, and the Viking Mars landers and orbiters, used as active retransmitters of the radar signals ("active radar').

The results for the coefficient $\frac{1}{2}(1+\gamma)$ of all radar time-delay measurements performed to date (including a measurement of the one-way time delay of signals from the millisecond pulsar PSR 1937+21) are shown in Figure 5 (see TEGP 7.2 for discussion and references). The Viking experiment resulted in a 0.1 percent measurement.

From the results of light-deflection experiments, we can conclude that the coefficient $\frac{1}{2}(1+\gamma)$ must be within at most 0.016 percent of unity. Scalar-tensor theories must have $\omega > 3300$ to be compatible with this constraint.

3.5 The Perihelion Shift of Mercury

The explanation of the anomalous perihelion shift of Mercury's orbit was another of the triumphs of GR. This had been an unsolved problem in celestial mechanics for over half a century, since the announcement by Le Verrier in 1859 that, after the perturbing effects of the planets on Mercury's orbit had been accounted for, and after the effect of the precession of the equinoxes on the astronomical coordinate system had been subtracted, there remained in the data an unexplained advance in the perihelion of Mercury. The modern value for this discrepancy is 43 arcseconds per century. A number of *ad hoc* proposals were made in an attempt to account for this excess, including, among others, the existence of new planet Vulcan near the Sun, a ring of planetoids, a solar quadrupole moment and a deviation from the inverse-square law of gravitation but none was successful. General relativity accounted for the anomalous shift in a natural way without disturbing the agreement with other planetary observations.

Parameter	Effect	Limit	Remarks
$\gamma - 1$	time delay	2×10^{-3}	Viking ranging
	light deflection	3×10^{-4}	VLBI
$\beta - 1$	perihelion shift	3×10^{-3}	$J_2 = 10^{-7}$ from helioseismology
	Nordtvedt effect	6×10^{-4}	$\eta = 4\beta - \gamma - 3$ assumed
ξ	Earth tides	10^{-3}	gravimeter data
α_1	orbital polarization	4×10^{-4}	Lunar laser ranging
		2×10^{-4}	PSR J2317+1439
α_2	spin precession	4×10^{-7}	solar alignment with ecliptic
α_3	pulsar acceleration	2×10^{-20}	pulsar $\dot{P}$ statistics
η[1]	Nordtvedt effect	10^{-3}	lunar laser ranging
ζ_1	–	2×10^{-2}	combined PPN bounds
ζ_2	binary acceleration	4×10^{-5}	$\ddot{P}_p$ for PSR 1913+16
ζ_3	Newton's 3rd law	10^{-8}	Lunar acceleration
ζ_4	–	–	not independent

[1]Here $\eta = 4\beta - \gamma - 3 - 10\xi/3 - \alpha_1 - 2\alpha_2/3 - 2\zeta_1/3 - \zeta_2/3$

Table 4. Current Limits on the PPN Parameters

The predicted advance, $\Delta\tilde{\omega}$, per orbit, including both relativistic PPN contributions and the Newtonian contribution resulting from a possible solar quadrupole moment, is given by

$$\Delta\tilde{\omega} = (6\pi m/p)[\frac{1}{3}(2+2\gamma-\beta)+\frac{1}{6}\,(2\alpha_1-\alpha_2+\alpha_3+2\zeta_2)\mu/m+J_2(R^2/2mp)]\,, \quad (35)$$

where $m \equiv m_1+m_2$ and $\mu \equiv m_1m_2/m$ are the total mass and reduced mass of the two-body system respectively; $p \equiv a(1-e^2)$ is the semi-latus rectum of the orbit, with a the semi-major axis and e the eccentricity; R is the mean radius of the oblate body; and J_2 is a dimensionless measure of its quadrupole moment, given by $J_2 = (C-A)/m_1R^2$, where C and A are the moments of inertia about the body's rotation and equatorial axes, respectively (for details of the derivation see TEGP 7.3). We have ignored preferred-frame and galaxy-induced contributions to $\Delta\tilde{\omega}$; these are discussed in TEGP 8.3.

The first term in Equation 35 is the classical relativistic perihelion shift, which depends upon the PPN parameters γ and β. The second term depends upon the ratio of the masses of the two bodies; it is zero in any fully conservative theory of gravity ($\alpha_1 \equiv \alpha_2 \equiv \alpha_3 \equiv \zeta_2 \equiv 0$); it is also negligible for Mercury, since $\mu/m \approx m_{\rm Merc}/m_\odot \approx 2\times10^{-7}$. We shall drop this term henceforth. The third term depends upon the solar quadrupole moment J_2. For a Sun that rotates uniformly with its observed surface angular velocity, so that the quadrupole moment is produced by centrifugal flattening, one may estimate J_2 to be $\sim 1\times10^{-7}$. This actually agrees reasonably well with values inferred from rotating solar models that are in accord with observations of the normal modes of solar oscillations (helioseismology). Substituting standard orbital elements and physical constants for Mercury and the Sun we obtain the rate of perihelion shift $\dot{\tilde{\omega}}$, in seconds of arc per century,

$$\dot{\tilde{\omega}} = 42.''98\left[\frac{1}{3}(2+2\gamma-\beta)+3\times10^{-4}(J_2/10^{-7})\right]\,. \quad (36)$$

Now, the measured perihelion shift of Mercury is known accurately: after the perturbing effects of the other planets have been accounted for, the excess shift is known to about 0.1 percent from radar observations of Mercury since 1966. The solar oblateness effect is smaller than the observational error, so we obtain the PPN bound $|2\gamma-\beta-1| < 3\times10^{-3}$.

3.6 Tests of the Strong Equivalence Principle

The next class of solar-system experiments that test relativistic gravitational effects may be called tests of the strong equivalence principle (SEP). In Sec. 3.1.2, we pointed out that many metric theories of gravity (perhaps all except GR) can be expected to violate one or more aspects of SEP. Among the testable violations of SEP are a violation of the weak equivalence principle for gravitating bodies that leads to perturbations in the Earth-Moon orbit; preferred-location and preferred-frame effects in the locally measured gravitational constant that could produce observable geophysical effects; and possible variations in the gravitational constant over cosmological timescales.

3.6.1 The Nordtvedt Effect and the Lunar Eötvös Experiment

In a pioneering calculation using his early form of the PPN formalism, Nordtvedt showed that many metric theories of gravity predict that massive bodies violate the weak equivalence principle–that is, fall with different accelerations depending on their gravitational self-energy. For a spherically symmetric body, the acceleration from rest in an external gravitational potential U has the form

$$\begin{aligned} \mathbf{a} &= (m_p/m)\nabla U\,, \\ m_p/m &= 1-\eta(E_g/m)\,, \\ \eta &= 4\beta-\gamma-3-\frac{10}{3}\xi-\alpha_1+\frac{2}{3}\alpha_2-\frac{2}{3}\zeta_1-\frac{1}{3}\zeta_2\,, \end{aligned} \tag{37}$$

where E_g is the negative of the gravitational self-energy of the body ($E_g > 0$). This violation of the massive-body equivalence principle is known as the "Nordtvedt effect". The effect is absent in GR ($\eta = 0$) but present in scalar-tensor theory ($\eta = 1/(2+\omega)+4\Lambda$). The existence of the Nordtvedt effect does not violate the results of laboratory Eötvös experiments, since for laboratory-sized objects, $E_g/m \leq 10^{-27}$, far below the sensitivity of current or future experiments. However, for astronomical bodies, E_g/m may be significant (10^{-5} for the Sun, 10^{-8} for Jupiter, 4.6×10^{-10} for the Earth, 0.2×10^{-10} for the Moon). If the Nordtvedt effect is present ($\eta \neq 0$) then the Earth should fall toward the Sun with a slightly different acceleration than the Moon. This perturbation in the Earth-Moon orbit leads to a polarization of the orbit that is directed toward the Sun as it moves around the Earth-Moon system, as seen from Earth. This polarization represents

a perturbation in the Earth-Moon distance of the form

$$\delta r = 13.1\eta \cos(\omega_0 - \omega_s)t \quad \text{m}\,, \tag{38}$$

where ω_0 and ω_s are the angular frequencies of the orbits of the Moon and Sun around the Earth (see TEGP 8.1, for detailed derivations and references; for improved calculations of the numerical coefficient, see Refs. 26,27).

Since August 1969, when the first successful acquisition was made of a laser signal reflected from the Apollo 11 retroreflector on the Moon, the lunar laser-ranging experiment (LURE) has made regular measurements of the round-trip travel times of laser pulses between a network of observatories and the lunar retroreflectors, with accuracies that are approaching 50 ps (1 cm). These measurements are fit using the method of least-squares to a theoretical model for the lunar motion that takes into account perturbations due to the Sun and the other planets, tidal interactions, and post-Newtonian gravitational effects. The predicted round-trip travel times between retroreflector and telescope also take into account the librations of the Moon, the orientation of the Earth, the location of the observatory, and atmospheric effects on the signal propagation. The "Nordtvedt" parameter η along with several other important parameters of the model are then estimated in the least-squares method.

Several independent analyses of the data found no evidence, within experimental uncertainty, for the Nordtvedt effect (for recent results see Ref. 28). Their results can be summarized by the bound $|\eta| < 0.001$. These results represent a limit on a possible violation of WEP for massive bodies of 5 parts in 10^{13} (compare Figure 1). For Brans-Dicke theory, these results force a lower limit on the coupling constant ω of 1000. Note that, at this level of precision, one cannot regard the results of lunar laser ranging as a "clean" test of SEP because the precision exceeds that of laboratory tests of WEP. Because the chemical compositions of the Earth and Moon differ in the relative fractions of iron and silicates, an extrapolation from laboratory Eötvös-type experiments to the Earth-Moon systems using various non-metric couplings to matter yields bounds on violations of WEP only of the order of 2×10^{-12}. Thus if lunar laser ranging is to test SEP at higher accuracy, tests of WEP must keep pace; to this end, a proposed satellite test of the equivalence principle (Sec. 2.3) will be an important advance.

In GR, the Nordtvedt effect vanishes; at the level of several centimeters and below, a number of non-null general relativistic effects should be present.[26]

3.6.2 Preferred-Frame and Preferred-Location Effects

Some theories of gravity violate SEP by predicting that the outcomes of local gravitational experiments may depend on the velocity of the laboratory relative to the mean rest frame of the universe (preferred-frame effects) or on the location of the laboratory relative to a nearby gravitating body (preferred-location effects). In the post-Newtonian limit, preferred-frame effects are governed by the values of the PPN parameters α_1, α_2, and α_3, and some preferred-location effects are governed by ξ (see Table 2).

The most important such effects are variations and anisotropies in the locally-measured value of the gravitational constant, which lead to anomalous Earth tides and variations in the Earth's rotation rate; anomalous contributions to the orbital dynamics of Mercury and Mars; self-accelerations of pulsars, and anomalous torques on the Sun that would cause its spin axis to be randomly oriented relative to the ecliptic (see TEGP 8.2, 8.3, 9.3 and 14.3(c)). An improved bound on α_3 of 2×10^{-20} from the period derivatives of 20 millisecond pulsars was reported in Ref. 29; an improved bound on α_1 was achieved using observations of the circular binary orbit of the pulsar J2317+1439 (Ref. 30). Negative searches for these effects have produced strong constraints on the PPN parameters (Table 4).

3.6.3 Constancy of the Newtonian Gravitational Constant

Most theories of gravity that violate SEP predict that the locally measured Newtonian gravitational constant may vary with time as the universe evolves. For the scalar-tensor theories listed in Table 3, the predictions for $\dot{G}/G$ can be written in terms of time derivatives of the asymptotic scalar field. Where G does change with cosmic evolution, its rate of variation should be of the order of the expansion rate of the universe, *i.e.*, $\dot{G}/G \sim H_0$, where H_0 is the Hubble expansion parameter and is given by $H_0 = 100h$ km s^{-1} Mpc^{-1} $= h \times 10^{-10}\,\mathrm{yr}^{-1}$, where current observations of the expansion of the universe give $\frac{1}{2} < h < 1$.

Several observational constraints can be placed on $\dot{G}/G$ using methods that include studies of the evolution of the Sun, observations of lunar occultations (including analyses of ancient eclipse data), lunar laser-ranging measurements, planetary radar-ranging measurements, and pulsar timing data. Laboratory experiments may one day lead to interesting limits (for review and references to past

Method	$\dot{G}/G(10^{-12}\ \mathrm{yr}^{-1})$
Lunar Laser Ranging	0 ± 8
Viking Radar	2 ± 4
	-2 ± 10
Binary Pulsar[1]	11 ± 11
Pulsar PSR 0655+64[1]	< 55

[1] Bounds dependent upon theory of gravity in strong-field regime and on neutron star equation of state.

Table 5. Constancy of the Gravitational Constant

work see TEGP 8.4 and 14.3(c)). Recent results are shown in Table 5.

The best limits on $\dot{G}/G$ still come from ranging measurements to the Viking landers and Lunar laser ranging measurements.[28] It has been suggested that radar observations of a Mercury orbiter over a two-year mission (30 cm accuracy in range) could yield $\Delta(\dot{G}/G) \sim 10^{-14}\ \mathrm{yr}^{-1}$.

Although bounds on $\dot{G}/G$ using solar-system measurements can be obtained in a phenomenological manner through the simple expedient of replacing G by $G_0 + \dot{G}_0(t - t_0)$ in Newton's equations of motion, the same does not hold true for pulsar and binary pulsar timing measurements. The reason is that, in theories of gravity that violate SEP, such as scalar-tensor theories, the "mass" and moment of inertia of a gravitationally bound body may vary with variation in G. Because neutron stars are highly relativistic, the fractional variation in these quantities can be comparable to $\Delta G/G$, the precise variation depending both on the equation of state of neutron star matter and on the theory of gravity in the strong-field regime. The variation in the moment of inertia affects the spin rate of the pulsar, while the variation in the mass can affect the orbital period in a manner that can add to or subtract from the direct effect of a variation in G, given by $\dot{P}_b/P_b = -\frac{1}{2}\dot{G}/G$. Thus, the bounds quoted in Table 5 for the binary pulsar PSR 1913+16 and the pulsar PSR 0655+64 are theory-dependent and must be treated as merely suggestive.

3.7 Other Tests of Post-Newtonian Gravity

3.7.1 Tests of Post-Newtonian Conservation Laws

Of the five "conservation law" PPN parameters ζ_1, ζ_2, ζ_3, ζ_4, and α_3, only three, ζ_2, ζ_3 and α_3, have been constrained directly with any precision; ζ_1 is constrained indirectly through its appearance in the Nordtvedt effect parameter η, Equation 37. There is strong theoretical evidence that ζ_4, which is related to the gravity generated by fluid pressure, is not really an independent parameter–in any reasonable theory of gravity there should be a connection between the gravity produced by kinetic energy (ρv^2), internal energy ($\rho\Pi$), and pressure (p). From such considerations, there follows[31] the additional theoretical constraint

$$6\zeta_4 = 3\alpha_3 + 2\zeta_1 - 3\zeta_3 \,. \tag{39}$$

A non-zero value for any of these parameters would result in a violation of conservation of momentum, or of Newton's third law in gravitating systems. An alternative statement of Newton's third law for gravitating systems is that the "active gravitational mass", that is the mass that determines the gravitational potential exhibited by a body, should equal the "passive gravitational mass", the mass that determines the force on a body in a gravitational field. Such an equality guarantees the equality of action and reaction and of conservation of momentum, at least in the Newtonian limit.

A classic test of Newton's third law for gravitating systems was carried out in 1968 by Kreuzer, in which the gravitational attraction of fluorine and bromine were compared to a precision of 5 parts in 10^5.

A remarkable planetary test was reported by Bartlett and van Buren. They noted that current understanding of the structure of the Moon involves an iron-rich, aluminum-poor mantle whose center of mass is offset about 10 km from the center of mass of an aluminum-rich, iron-poor crust. The direction of offset is toward the Earth, about 14° to the east of the Earth-Moon line. Such a model accounts for the basaltic maria which face the Earth, and the aluminum-rich highlands on the Moon's far side, and for a 2 km offset between the observed center of mass and center of figure for the Moon. Because of this asymmetry, a violation of Newton's third law for aluminum and iron would result in a momentum non-conserving self-force on the Moon, whose component along the orbital direction would contribute to the secular acceleration of the lunar orbit. Improved knowl-

edge of the lunar orbit through lunar laser ranging, and a better understanding of tidal effects in the Earth-Moon system (which also contribute to the secular acceleration) through satellite data, severely limit any anomalous secular acceleration, with the resulting limit

$$\left|\frac{(m_A/m_P)_{\rm Al} - (m_A/m_P)_{\rm Fe}}{(m_A/m_P)_{\rm Fe}}\right| < 4 \times 10^{-12} \,. \tag{40}$$

According to the PPN formalism, in a theory of gravity that violates conservation of momentum, but that obeys the constraint of Equation 39, the electrostatic binding energy E_e of an atomic nucleus could make a contribution to the ratio of active to passive mass of the form

$$m_A = m_P + \frac{1}{2}\zeta_3 E_e/c^2 \,. \tag{41}$$

The resulting limits on ζ_3 from the lunar experiment is $\zeta_3 < 1 \times 10^{-8}$ (TEGP 9.2, 14.3(d)).

Another consequence of a violation of conservation of momentum is a self-acceleration of the center of mass of a binary stellar system, given by

$$\mathbf{a}_{\rm CM} = \frac{1}{2}(\zeta_2 + \alpha_3)\frac{m}{a^2}\frac{\mu}{a}\frac{\delta m}{m}\frac{e}{(1-e^2)^{3/2}}\mathbf{n}_P \,, \tag{42}$$

where $\delta m = m_1 - m_2$, a is the semi-major axis, and $\mathbf{n}_P$ is a unit vector directed from the center of mass to the point of periastron of m_1 (TEGP 9.3). A consequence of this acceleration would be non-vanishing values for d^2P/dt^2, where P denotes the period of any intrinsic process in the system (orbit, spectra, pulsar periods). The observed upper limit on d^2P_p/dt^2 of the binary pulsar PSR 1913+16 places a strong constraint on such an effect, resulting in the bound $|\alpha_3 + \zeta_2| < 4 \times 10^{-5}$. Since α_3 has already been constrained to be much less than this (Table 4), we obtain a strong bound on ζ_2 alone.[32]

3.7.2 Geodetic Precession

A gyroscope moving through curved spacetime suffers a precession of its axis given by

$$d\mathbf{S}/d\tau = \mathbf{\Omega}_G \times \mathbf{S} \,, \qquad \mathbf{\Omega}_G = (\gamma + \frac{1}{2})\mathbf{v} \times \nabla U \,, \tag{43}$$

where $\mathbf{v}$ is the velocity of the gyroscope, and U is the Newtonian gravitational potential of the source (TEGP 9.1). The Earth-Moon system can be considered

as a "gyroscope", with its axis perpendicular to the orbital plane. The predicted precession is about 2 arcseconds per century, an effect first calculated by de Sitter. This effect has been measured to about 0.7 percent using Lunar laser ranging data.[28]

For a gyroscope orbiting the Earth, the precession is about 8 arcseconds per year. The Stanford Gyroscope Experiment has as one of its goals the measurement of this effect to 5×10^{-5} (see below).

3.7.3 Search for Gravitomagnetism

According to GR, moving or rotating matter should produce a contribution to the gravitational field that is the analogue of the magnetic field of a moving charge or a magnetic dipole. Although gravitomagnetism plays a role in a variety of measured relativistic effects, it has not been seen to date, isolated from other post-Newtonian effects. The Relativity Gyroscope Experiment (Gravity Probe B or GP-B) at Stanford University, in collaboration with NASA and Lockheed-Martin Corporation, is in the advanced stage of developing a space mission to detect this phenomenon directly.[33] A set of four superconducting-niobium-coated, spherical quartz gyroscopes will be flown in a low polar Earth orbit, and the precession of the gyroscopes relative to the distant stars will be measured. In the PPN formalism, the predicted effect of gravitomagnetism is a precession (also known as the Lense-Thirring effect, or the dragging of inertial frames), given by

$$d\mathbf{S}/d\tau = \mathbf{\Omega}_{\rm LT} \times \mathbf{S}\,, \qquad \mathbf{\Omega}_{\rm LT} = -\frac{1}{2}(1+\gamma+\frac{1}{4}\alpha_1)[\mathbf{J} - 3\mathbf{n}(\mathbf{n}\cdot\mathbf{J})]/r^3\,, \qquad (44)$$

where $\mathbf{J}$ is the angular momentum of the Earth, $\mathbf{n}$ is a unit radial vector, and r is the distance from the center of the Earth (TEGP 9.1). For a polar orbit at about 650 km altitude, this leads to a secular angular precession at a rate $\frac{1}{2}(1+\gamma+\frac{1}{4}\alpha_1)42 \times 10^{-3}$ arcsec/yr. The accuracy goal of the experiment is about 0.5 milliarcseconds per year. The science instrument package and the spacecraft are in the final phases of construction, with launch scheduled for early 2000.

Another proposal to look for an effect of gravitomagnetism is to measure the relative precession of the line of nodes of a pair of laser-ranged geodynamics satellites (LAGEOS), ideally with supplementary inclination angles; the inclinations must be supplementary in order to cancel the dominant nodal precession caused by the Earth's Newtonian gravitational multipole moments. Unfortunately, the two

existing LAGEOS satellites are not in appropriately inclined orbits, and no plans exist at present to launch a third satellite in a supplementary orbit. Nevertheless, by combing nodal precession data from LAGEOS I and II with perigee advance data from the slightly eccentric orbit of LAGEOS II, Ciufolini *et al.* reported a partial cancellation of multipole effects, and a resulting 20 percent confirmation of GR.[34]

3.7.4 Improved PPN Parameter Values

A number of advanced space missions have been proposed in which spacecraft orbiters or landers and improved tracking capabilities could lead to significant improvements in values of the PPN parameters, of J_2 of the Sun, and of $\dot{G}/G$. For example, a Mercury orbiter, in a two-year experiment, with 3 cm range capability, could yield improvements in the perihelion shift to a part in 10^4, in γ to 4×10^{-5}, in $\dot{G}/G$ to 10^{-14} yr^{-1}, and in J_2 to a few parts in 10^8. Proposals are being developed, primarily in Europe, for advanced space missions which will have tests of PPN parameters as key components, including GAIA, a high-precision astrometric telescope (successor to Hipparcos), which could measure light-deflection and γ to the 10^{-6} level, and a solar orbit relativity test, which could measure γ to 10^{-7} from time delay and light deflection measurements.

3.7.5 Gravitational-Wave Astronomy

A significant part of the field of experimental gravitation is devoted to building and designing sensitive devices to detect gravitational radiation and to use gravity waves as a new astronomical tool. The centerpieces of this effort are the US Laser Interferometric Gravitational-wave Observatory (LIGO) and the European VIRGO projects, which are currently under construction. This important topic has been reviewed thoroughly elsewhere,[35] and in this volume.

4 Stellar System Tests of Gravitational Theory

4.1 Binary Pulsars and General Relativity

The majority of tests of gravitational theory described so far have involved solar-system dynamics or laboratory experiments. Although the results confirm GR,

they test only a limited portion of the "space of predictions" of a theory. This portion corresponds to the weak-field, slow-motion, post-Newtonian limit. The 1974 discovery of the binary pulsar PSR 1913+16 by Taylor and Hulse opened up the possibility of probing new aspects of gravitational theory: the effects of strong relativistic internal gravitational fields on orbital dynamics, and the effects of gravitational radiation reaction. For reviews of the discovery and current status, see the published Nobel Prize lectures by Hulse and Taylor.[36,37]

The system consists of a pulsar of nominal period 59 ms in a close binary orbit with an as yet unseen companion. From detailed analyses of the arrival times of pulses (which amounts to an integrated version of the Doppler-shift methods used in spectroscopic binary systems), extremely accurate orbital and physical parameters for the system have been obtained (Table 6). Because the orbit is so close ($\approx 1 R_\odot$) and because there is no evidence of an eclipse of the pulsar signal or of mass transfer from the companion, it is generally believed that the companion is compact: evolutionary arguments suggest that it is most likely a dead pulsar. Thus the orbital motion is very clean, free from tidal or other complicating effects. Furthermore, the data acquisition is "clean" in the sense that the observers can keep track of the pulsar phase with an accuracy of 15μs, despite gaps of up to six months between observing sessions. The pulsar has shown no evidence of "glitches" in its pulse period.

Three factors make this system an arena where relativistic celestial mechanics must be used: the relatively large size of relativistic effects [$v_{\rm orbit} \approx (m/r)^{1/2} \approx 10^{-3}$]; the short orbital period (8 hours), allowing secular effects to build up rapidly; and the cleanliness of the system, allowing accurate determinations of small effects. Just as Newtonian gravity is used as a tool for measuring astrophysical parameters of ordinary binary systems, so GR is used as a tool for measuring astrophysical parameters in the binary pulsar.

The observational parameters that are obtained from a least squares solution of the arrival time data fall into three groups: (i) non-orbital parameters, such as the pulsar period and its rate of change, and the position of the pulsar on the sky; (ii) five "Keplerian" parameters, most closely related to those appropriate for standard Newtonian systems, such as the eccentricity e and the orbital period P_b; and (iii) five "post-Keplerian" parameters. The five post-Keplerian parameters are $\langle\dot\omega\rangle$, the average rate of periastron advance; γ', the amplitude of delays in arrival of pulses caused by the varying effects of the gravitational redshift and

Parameter	Symbol (units)	Value[1]
(i) **"Physical" Parameters**		
Right Ascension	α	$19^h15^m28.^s00018(15)$
Declination	δ	$16°06'27.''4043(3)$
Pulsar Period	P_p (ms)	59.029997929613(7)
Derivative of Period	$\dot{P}_p$	$8.62713(8) \times 10^{-18}$
(ii) **"Keplerian" Parameters**		
Projected semimajor axis	$a_p \sin i$ (s)	2.3417592(19)
Eccentricity	e	0.6171308(4)
Orbital Period	P_b (day)	0.322997462736(7)
Longitude of periastron	ω_0 (°)	226.57528(6)
Julian ephemeris date of periastron	T_0 (MJD)	46443.99588319(3)
(iii) **"Post-Keplerian" Parameters**		
Mean rate of periastron advance	$\langle\dot{\omega}\rangle$ ($^\circ$ yr^{-1})	4.226621(11)
Gravitational redshift/time dilation	γ' (ms)	4.295(2)
Orbital period derivative	$\dot{P}_b\,(10^{-12})$	$-2.422(6)$

[1]Numbers in parentheses denote errors in last digit.

Table 6. Parameters of the Binary Pulsar PSR 1913+16

time dilation as the pulsar moves in its elliptical orbit at varying distances from the companion and with varying speeds; $\dot{P}_b$, the rate of change of orbital period, caused predominantly by gravitational radiation damping; and r and $s = \sin i$, respectively the "range" and "shape" of the Shapiro time delay caused by the companion, where i is the angle of inclination of the orbit relative to the plane of the sky.

In GR, these post-Keplerian parameters can be related to the masses of the two bodies and to measured Keplerian parameters by the equations (TEGP 12.1, 14.6(a))

$$\langle \dot{\omega} \rangle = 3(2\pi/P_b)^{5/3} m^{2/3} (1-e^2)^{-1} , \quad (45)$$

$$\gamma' = e(P_b/2\pi)^{1/3} m_2 m^{-1/3} (1 + m_2/m) , \quad (46)$$

$$\dot{P}_b = -(192\pi/5)(2\pi m/P_b)^{5/3} (\mu/m) \left(1 + \frac{73}{24}e^2 + \frac{37}{96}e^4\right) (1-e^2)^{-7/2} , \quad (47)$$

$$s = \sin i , \quad (48)$$

$$r = m_2 , \quad (49)$$

where m_1 and m_2 denote the pulsar and companion masses, respectively. The formula for $\langle \dot{\omega} \rangle$ ignores possible non-relativistic contributions to the periastron shift, such as tidally or rotationally induced effects caused by the companion (for discussion of these effects, see TEGP 12.1(c)). The formula for $\dot{P}_b$ represents the effect of energy loss through the emission of gravitational radiation, and makes use of the "quadrupole formula" of GR (for a survey of the quadrupole and other approximations for gravitational radiation, see Ref. 38); it ignores other sources of energy loss, such as tidal dissipation (TEGP 12.1(f)).

The timing model that contains these parameters was developed by Damour, Deruelle and Taylor, superseding earlier treatments by Haugan, Blandford, Teukolsky and Epstein. The current values for Keplerian and post-Keplerian parameters are shown in Table 6.

The most convenient way to display these results is to plot the constraints they imply for the two masses m_1 and m_2, via Equations 45 and 46. These are shown in Figure 6. From $\langle \dot{\omega} \rangle$ and γ' we obtain the values $m_1 = 1.4411 \pm 0.0007 M_\odot$ and $m_2 = 1.3873 \pm 0.0007 M_\odot$. Equation 47 then predicts the value $\dot{P}_b = -2.40243 \pm 0.00005 \times 10^{-12}$. In order to compare the predicted value for $\dot{P}_b$ with the observed value, it is necessary to take into account the effect of a relative acceleration between the binary pulsar system and the solar system caused by the differential

rotation of the galaxy. This effect was previously considered unimportant when $\dot{P}_b$ was known only to 10 percent accuracy. Damour and Taylor carried out a careful estimate of this effect using data on the location and proper motion of the pulsar, combined with the best information available on galactic rotation, and found

$$\dot{P}_b^{\rm GAL} \simeq -(1.7 \pm 0.5) \times 10^{-14} \,. \tag{50}$$

Subtracting this from the observed $\dot{P}_b$ (Table 5) gives the residual

$$\dot{P}_b^{\rm OBS} = -(2.408 \pm 0.010[{\rm OBS}] \pm 0.005[{\rm GAL}]) \times 10^{-12} \,, \tag{51}$$

which agrees with the prediction, within the errors. In other words,

$$\frac{\dot{P}_b^{\rm GR}}{\dot{P}_b^{\rm OBS}} = 1.0023 \pm 0.0041[{\rm OBS}] \pm 0.0021[{\rm GAL}] \,. \tag{52}$$

The parameters r and s are not separately measurable with interesting accuracy for PSR 1913+16 because the orbit's 47° inclination does not lead to a substantial Shapiro delay.

The consistency among the measurements is also displayed in Figure 6, in which the regions allowed by the three most precise constraints have a single common overlap. This consistency provides a test of the assumption that the two bodies behave as "point" masses, without complicated tidal effects, obeying the general relativistic equations of motion including gravitational radiation. It is also a test of the strong equivalence principle, in that the highly relativistic internal structure of the neutron star does not influence its orbital motion, as predicted by GR. Recent observations[39] indicate variations in the pulse profile, which suggests that the pulsar is undergoing geodetic precession (Sec. 3.7.2) in an amount consistent with GR, assuming that the pulsar's spin is suitably misaligned with the orbital angular momentum.

4.2 A Population of Binary Pulsars?

Since 1990, several new massive binary pulsars similar to PSR 1913+16 were discovered, leading to the possibility of new or improved tests of GR.

PSR 1534+12. This is a binary pulsar system in our galaxy. Its pulses are significantly stronger and narrower than those of PSR 1913+16, so timing measurements are more precise, reaching $3\mu s$ accuracy. Its parameters are listed

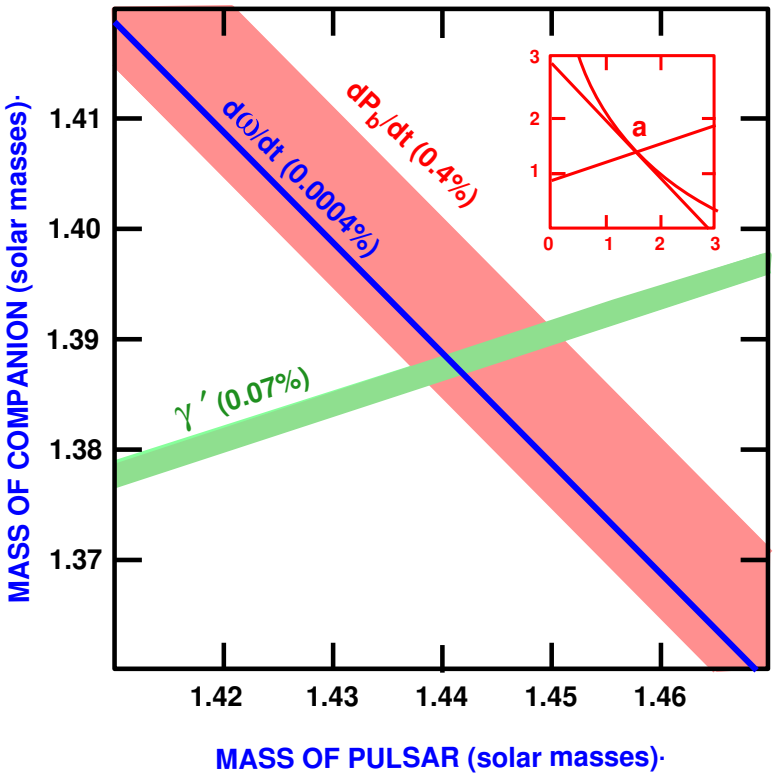

Fig. 6. Constraints on masses of pulsar and companion from data on PSR 1913+16, assuming GR to be valid. Width of each strip in the plane reflects observational accuracy, shown as a percentage. Inset shows the three constraints on the full mass plane; intersection region (a) has been magnified 400 times for the full figure.

Parameter	B1534+12	B2127+11C	B1855+09
(i) "Keplerian" Parameters			
$a_p \sin i$ (s)	3.729463(3)	2.520(3)	9.2307802(4)
e	0.2736777(5)	0.68141(2)	0.00002168(5)
P_b(day)	0.42073729929(4)	0.335282052(6)	12.3271711905(6)
(ii) "Post-Keplerian" Parameters[1]			
$\langle\dot{\omega}\rangle\,(^\circ\,\mathrm{yr}^{-1})$	1.75576(4)	4.457(12)	
γ' (ms)	2.066(10)	4.9(1.1)	
$\dot{P}_b\,(10^{-12})$	$-0.129(14)$		
$r(\mu\mathrm{s})$	6.7(1.3)		1.27(10)
$s = \sin i$	0.982(7)		0.9992(5)

[1] From Ref. 40,41 and http://puppsr8.princeton.edu/psrcat.html

Table 7. Parameters of New Binary Pulsars

in Table 6.[41] The orbital plane appears to be almost edge-on relative to the line of sight ($i \simeq 80^\circ$); as a result the Shapiro delay is substantial, and separate values of the parameters r and s have been obtained with interesting accuracy. Assuming general relativity, one infers that the two masses are virtually identical at $1.339 \pm 0.003 M_\odot$. The rate of orbit decay $\dot{P}_b$ agrees with GR to about 15 percent, the precision limited by the poorly known distance to the pulsar, which introduces a significant uncertainty into the subtraction of galactic acceleration.

PSR 2127+11C. This system appears to be a clone of the Hulse-Taylor binary pulsar, with very similar values for orbital period and eccentricity (see Table 7). The inferred total mass of the system is $2.706 \pm 0.011 M_\odot$. Because the system is in the globular cluster M15 (NGC 7078), it will suffer Doppler shifts resulting from local accelerations, either by the mean cluster gravitational field or by nearby stars, that are more difficult to estimate than was the case with the galactic system PSR 1913+16. This may make a separate, precision measurement of the relativistic contribution to $\dot{P}_b$ impossible.

PSR 1855+09. This binary pulsar system is not particularly relativistic, with a long period (12 days) and highly circular orbit. However, because we observe the orbit nearly edge on, the Shapiro delay is large and measurable, as reflected in the post-Keplerian parameters r and s.

4.3 Binary Pulsars and Alternative Theories

Soon after the discovery of the binary pulsar it was widely hailed as a new testing ground for relativistic gravitational effects. As we have seen in the case of GR, in most respects, the system has lived up to, indeed exceeded, the early expectations.

In another respect, however, the system has only partially lived up to its promise, namely as a direct testing ground for alternative theories of gravity. The origin of this promise was the discovery that alternative theories of gravity generically predict the emission of dipole gravitational radiation from binary star systems. This additional form of gravitational radiation damping could, at least in principle, be significantly stronger than the usual quadrupole damping, because it depends on fewer powers of the parameter v/c, where v is the orbital velocity and c is the speed of light, and it depends on the gravitational binding energy per unit mass of the bodies, which, for neutron stars, could be as large as 40 per cent. As one fulfillment of this promise, Will and Eardley worked out in detail the effects of dipole gravitational radiation in the bimetric theory of Rosen, and, when the first observation of the decrease of the orbital period was announced in 1978, the Rosen theory suffered a terminal blow (TEGP 12.3). A wide class of alternative theories also fail the binary pulsar test because of dipole gravitational radiation.

On the other hand, the early observations already indicated that, in GR, the masses of the two bodies were nearly equal, so that, in theories of gravity that are in some sense "close" to GR, dipole gravitational radiation would not be a strong effect, because of the apparent symmetry of the system (technically, the amount of dipole radiation depends on the difference between the gravitational binding energy per unit mass for the two bodies). The Rosen theory, and others like it, are not "close" to general relativity, except in their predictions for the weak-field, slow-motion regime of the solar system. When relativistic neutron stars are present, theories like these can predict strong effects on the motion of the bodies resulting from their internal highly relativistic gravitational structure (violations of the Strong Equivalence Principle). As a consequence, the masses inferred from observations such as the periastron shift may be significantly different from those inferred using general relativity, and may be different from each other, leading to strong dipole gravitational radiation damping. By contrast, the Brans-Dicke theory, which was the basis for Eardley's discovery of the dipole radiation phe-

nomenon, is "close" to GR, roughly speaking within $1/\omega_{\rm BD}$ of the predictions of the latter, for large values of the coupling constant $\omega_{\rm BD}$ (henceforth this notation for the coupling constant is adopted to avoid confusion with the periastron angle). Thus, despite the presence of dipole gravitational radiation, the binary pulsar provides at present only a weak test of Brans-Dicke theory, not yet competitive with solar-system tests.

4.4 Binary Pulsars and Scalar-Tensor Theories

Making the usual assumption that both members of the system are neutron stars, and using the methods summarized in TEGP Chapters 10–12, one can obtain formulas for the periastron shift, the gravitational redshift/second-order Doppler shift parameter, and the rate of change of orbital period, analogous to Equations 45–47. These formulas depend on the masses of the two neutron stars, on their self-gravitational binding energy, represented by "sensitivities" s and κ^* and on the Brans-Dicke coupling constant $\omega_{\rm BD}$. First, there is a modification of Kepler's third law, given by

$$P_b/2\pi = (a^3/\mathcal{G}m)^{1/2}\,. \tag{53}$$

Then, the predictions for $\langle\dot\omega\rangle$, γ' and $\dot P_b$ are

$$\begin{aligned}
\langle\dot\omega\rangle &= 3(2\pi/P_b)^{5/3}m^{2/3}(1-e^2)^{-1}\mathcal{P}\mathcal{G}^{-4/3}\,, &(54)\\
\gamma' &= e(P_b/2\pi)^{1/3}m_2m^{-1/3}\mathcal{G}^{-1/3}(\alpha_2^*+\mathcal{G}m_2/m+\kappa_1^*\eta_2^*)\,, &(55)\\
\dot P_b &= -(192\pi/5)(2\pi m/P_b)^{5/3}(\mu/m)\mathcal{G}^{-4/3}F(e)\\
&\quad -4\pi(2\pi m/P_b)(\mu/m)\xi\mathcal{S}^2G(e)\,, &(56)
\end{aligned}$$

where, to first order in $\xi\equiv(2+\omega_{\rm BD})^{-1}$, we have

$$\begin{aligned}
F(e) &= \frac{1}{12}(1-e^2)^{-7/2}[\kappa_1(1+\frac{7}{2}e^2+\frac{1}{2}e^4)-\kappa_2(\frac{1}{2}e^2+\frac{1}{8}e^4)]\,, &(57)\\
G(e) &= (1-e^2)^{-5/2}(1+\frac{1}{2}e^2)\,, &(58)\\
\mathcal{S} &= s_1-s_2\,, &(59)\\
\mathcal{G} &= 1-\xi(s_1+s_2-2s_1s_2)\,, &(60)\\
\mathcal{P} &= \mathcal{G}[1-\frac{2}{3}\xi+\frac{1}{3}\xi(s_1+s_2-2s_1s_2)]\,, &(61)\\
\alpha_2^* &= 1-\xi s_2\,, &(62)\\
\eta_2^* &= (1-2s_2)\xi\,, &(63)
\end{aligned}$$

$$\kappa_1 = \mathcal{G}^2[12(1-\frac{1}{2}\xi)+\xi\Gamma^2]\,, \tag{64}$$

$$\kappa_2 = \mathcal{G}^2[11(1-\frac{1}{2}\xi)+\frac{1}{2}\xi(\Gamma^2-5\Gamma\Gamma'-\frac{15}{2}\Gamma'^2)]\,, \tag{65}$$

$$\Gamma = 1-2(m_1 s_2+m_2 s_1)/m\,, \tag{66}$$

$$\Gamma' = 1-s_1-s_2\,. \tag{67}$$

The quantities s_a and κ_a^* are defined by

$$s_a = -\left(\frac{\partial(\ln m_a)}{\partial(\ln G)}\right)_N\,, \qquad \kappa_a^* = -\left(\frac{\partial(\ln I_a)}{\partial(\ln G)}\right)_N\,, \tag{68}$$

and measure the "sensitivity" of the mass m_a and moment of inertia I_a of each body to changes in the scalar field (reflected in changes in G) for a fixed baryon number N (see TEGP 11, 12 and 14.6(c) for further details).

The first term in $\dot{P}_b$ (Equation 56) is the effect of quadrupole and monopole gravitational radiation, while the second term is the effect of dipole radiation. Equations 53–59 are quite general, applying to a class of "conservative" theories of gravity whose equations of motion for compact objects can be described by a Lagrangian (TEGP 11.3). The forms of the variables in the remaining equations are specific to Brans-Dicke theory.

In order to estimate the sensitivities s_1, s_2, $\mathcal{S}$ and κ^*, we must adopt an equation of state for the neutron stars. We restrict attention to relatively stiff neutron star equations of state in order to guarantee neutron stars of sufficient mass, approximately $1.4M_\odot$; the M and O equations of state of Arnett and Bowers give similar results. The lower limit on $\omega_{\rm BD}$ required to give consistency among the constraints on $\langle\dot{\omega}\rangle$, γ and $\dot{P}_b$ as in Figure 6 is 105. The combination of $\langle\dot{\omega}\rangle$ and γ give a constraint on the masses that is relatively weakly dependent on ξ, thus the constraint on ξ is dominated by $\dot{P}_b$ and is directly proportional to the measurement error in $\dot{P}_b$; in order to achieve a constraint comparable to the solar system value of 3×10^{-4}, the error in $\dot{P}_b^{\rm OBS}$ would have to be reduced by more than a factor of ten.

Damour and Esposito-Farèse[20] have devised a scalar-tensor theory in which two scalar fields are tuned so that their effects in the weak-field slow-motion regime of the solar system are suppressed, so that the theory is identical to general relativity in the post-Newtonian approximation. Yet in the regime appropriate to binary pulsars, it predicts strong-field SEP-violating effects and radiative effects that distinguish it from GR. It gives formulae for the post-Keplerian parameters

of Equations 54–56 as well as for the parameters r and s that have corrections dependent upon the sensitivities of the relativistic neutron stars. The theory depends upon two arbitrary parameters β' and β''; GR corresponds to the values $\beta'=\beta''=0$. It turns out that the binary pulsar PSR 1913+16 alone constrains the two parameters to a narrow but long strip in the (β', β'')-plane that includes the origin (GR) but that could include some highly non-general relativistic theories. The sensitivity of PSR 1534+12 to r and s provides an orthogonal constraint that cuts the strip. In this class of theories, then, *both* binary pulsars are needed to provide a strong test. Interestingly, it is the strong-field aspects of PSR 1534+12, not gravitational radiation, that provide the non-trivial new constraint. In scalar-tensor theories subject to "spontaneous-scalarization" in neutron-star interiors, the bounds from binary pulsars can be significantly stronger than those from the solar-system.[23]

5 Gravitational-Radiation Tests of Gravitational Theory

5.1 Laser-Interferometric Gravitational Observatories

Some time in the next decade, a new opportunity for testing relativistic gravity may be realized, with the completion and operation of kilometer-scale, laser interferometric gravitational-wave observatories in the U.S. (LIGO project), Europe (VIRGO and GEO-600 projects) and Japan (TAMA 300 project). Gravitational-wave searches at these observatories are scheduled to commence around 2002. The LIGO broad-band antennae will have the capability of detecting and measuring the gravitational waveforms from astronomical sources in a frequency band between about 10 Hz (the seismic noise cutoff) and 500 Hz (the photon counting noise cutoff), with a maximum sensitivity to strain at around 100 Hz of $\Delta l/l \sim 10^{-22}$ (rms). The most promising source for detection and study of the gravitational-wave signal is the "inspiralling compact binary" – a binary system of neutron stars or black holes (or one of each) in the final minutes of a death dance leading to a violent merger. Such is the fate, for example of the Hulse-Taylor binary pulsar PSR 1913+16 in about 300 M years. Given the expected sensitivity of the "advanced LIGO" (around 2007), which could see such sources out to hundreds of

megaparsecs, it has been estimated that from 3 to 100 annual inspiral events could be detectable. Other sources, such as supernova core collapse events, instabilities in rapidly rotating nascent neutron stars, signals from non-axisymmetric pulsars, and a stochastic background of waves, may be detectable (for reviews, see Ref. 35 and articles in this volume).

Detailed observation of gravitational waves from such sources may provide the means to test general relativistic predictions for the polarization and speed of the waves, and for gravitational radiation damping.

Several of these tests can be realized using gravitational-waves from inspiralling compact binaries. The analysis of gravitational-wave data from such sources will involve some form of matched filtering of the noisy detector output against an ensemble of theoretical "template" waveforms which depend on the intrinsic parameters of the inspiralling binary, such as the component masses, spins, and so on, and on its inspiral evolution. How accurate must a template be in order to "match" the waveform from a given source (where by a match we mean maximizing the cross-correlation or the signal-to-noise ratio)? In the total accumulated phase of the wave detected in the sensitive bandwidth, the template must match the signal to a fraction of a cycle. For two inspiralling neutron stars, around 16,000 cycles should be detected; this implies a phasing accuracy of 10^{-5} or better. Since $v/c \sim 1/10$ during the late inspiral, this means that correction terms in the phasing at the level of $(v/c)^5$ or higher are needed. More formal analyses confirm this intuition.[42]

Because it is a slow-motion system ($v/c \sim 10^{-3}$), the binary pulsar is sensitive only to the lowest-order effects of gravitational radiation as predicted by the quadrupole formula. Nevertheless, the first correction terms of order v/c and $(v/c)^2$ to the quadrupole formula, were calculated as early as 1976 (TEGP 10.3). These are now conventionally called "post-Newtonian" (PN) corrections, with each power of v/c corresponding to half a post-Newtonian order (1/2PN), in analogy with post-Newtonian corrections to the Newtonian equations of motion.[43]

But for laser-interferometric observations of gravitational waves, the bottom line is that, in order to measure the astrophysical parameters of the source and to test the properties of the gravitational waves, it is necessary to derive the gravitational waveform and the resulting radiation back-reaction on the orbit phasing at least to 2PN, or second post-Newtonian order, $O[(v/c)^4]$, beyond the quadrupole approximation, and probably to 3PN order.

5.2 Post-Newtonian Generation of Gravitational Waves

The generation of gravitational radiation is a long-standing problem that dates back to the first years following the publication of GR, when Einstein calculated the gravitational radiation emitted by a laboratory-scale object using the linearized version of GR. Shortly after the discovery of the binary pulsar PSR 1913+16 in 1974, questions were raised about the foundations of the "quadrupole formula" for gravitational radiation damping (and in some quarters, even about its quantitative validity). These questions were answered in part by theoretical work designed to shore up the foundations of the quadrupole approximation,[44] and in part (perhaps mostly) by the agreement between the predictions of the quadrupole formula and the *observed* rate of damping of the pulsar's orbit. In 1976, the post-Newtonian corrections to the quadrupole formula were of purely academic, rather than observational interest.

The challenge of providing accurate templates for LIGO-VIRGO data analysis has led to major efforts to calculate gravitational waves to high PN order. Three approaches have been developed.

The BDI approach of Blanchet, Damour and Iyer is based on a mixed post-Newtonian and "post-Minkowskian" framework for solving Einstein's equations approximately, developed in a long series of papers by Damour and colleagues.[45] The idea is to solve the vacuum Einstein equations in the exterior of the material sources extending out to the radiation zone in an expansion ("post-Minkowskian") in "nonlinearity" (effectively an expansion in powers of Newton's constant G), and to express the asymptotic solutions in terms of a set of formal, time-dependent, symmetric and trace-free (STF) multipole moments.[46] Then, in a near zone within one characteristic wavelength of the radiation, the equations including the material source are solved in a slow-motion approximation (expansion in powers of $1/c$) that yields a set of STF source multipole moments expressed as integrals over the "effective" source, including both matter and gravitational field contributions. The solutions involving the two sets of moments are then matched in an intermediate zone, resulting in a connection between the formal radiative moments and the source moments. The matching also provides a natural way, using analytic continuation, to regularize integrals involving the non-compact contributions of gravitational stress-energy, that might otherwise be divergent.

An approach called DIRE is based on a framework developed by Epstein and

Wagoner (EW),[47] and extended by Will, Wiseman and Pati. We shall describe DIRE briefly below.

A third approach, valid only in the limit in which one mass is much smaller than the other, is that of black-hole perturbation theory. This method provides numerical results that are exact in v/c, as well as analytical results expressed as series in powers of v/c, both for non-rotating and for rotating black holes. For non-rotating holes, the analytical expansions have been carried to *5.5* PN order.[48] In all cases of suitable overlap, the results of all three methods agree precisely.

5.2.1 Direct Integration of the Relaxed Einstein Equations (DIRE)

Like the BDI approach, DIRE involves rewriting the Einstein equations in their "relaxed" form, namely as an inhomogeneous, flat-spacetime wave equation for a field $h^{\alpha\beta}$, whose formal solution can be written

$$h^{\alpha\beta}(t,\mathbf{x}) = \quad 4\int_{\mathcal{C}} \frac{\tau^{\alpha\beta}(t-|\mathbf{x}-\mathbf{x}'|,\mathbf{x}')}{|\mathbf{x}-\mathbf{x}'|} d^3x' \ . \tag{69}$$

where the source $\tau^{\alpha\beta}$ consists of both the material stress-energy, and a "gravitational stress-energy" made up of all the terms non-linear in $h^{\alpha\beta}$, and the integration is over the past flat-spacetime null-cone $\mathcal{C}$ of the field point $(t,\mathbf{x})$ (see Fig. 7). The wave equation is accompanied by a harmonic or deDonder gauge condition $h^{\alpha\beta}{}_{,\beta} = 0$, which serves to specify a coordinate system, and also imposes equations of motion on the sources. Unlike the BDI approach, a *single* formal solution is written down, valid everywhere in spacetime. This formal solution, is then iterated in a slow-motion ($v/c < 1$), weak-field ($||h^{\alpha\beta}|| < 1$) approximation, that is very similar to the corresponding procedure in electromagnetism. However, because the integrand of this retarded integral is not compact by virture of the non-linear field contributions, the original EW formalism quickly runs up against integrals that are not well defined, or worse, are divergent. Although at the lowest quadrupole and first few PN orders, various arguments can be given to justify sweeping such problems under the rug,[49] they are not very rigorous, and provide no guarantee that the divergences do not become insurmountable at higher orders. As a consequence, despite efforts to cure the problem, the EW formalism fell into some disfavor as a route to higher orders, although an extension to 3/2PN order was accomplished.[50]

The resolution of this problem involves taking literally the statement that the

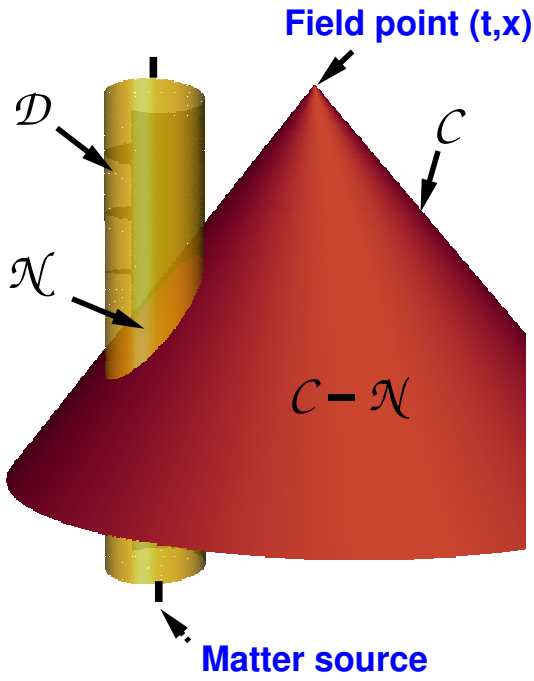

Fig. 7. Past harmonic null cone $\mathcal{C}$ of the field point $(t, \mathbf{x})$ intersects the near zone $\mathcal{D}$ in the hypersurface $\mathcal{N}$.

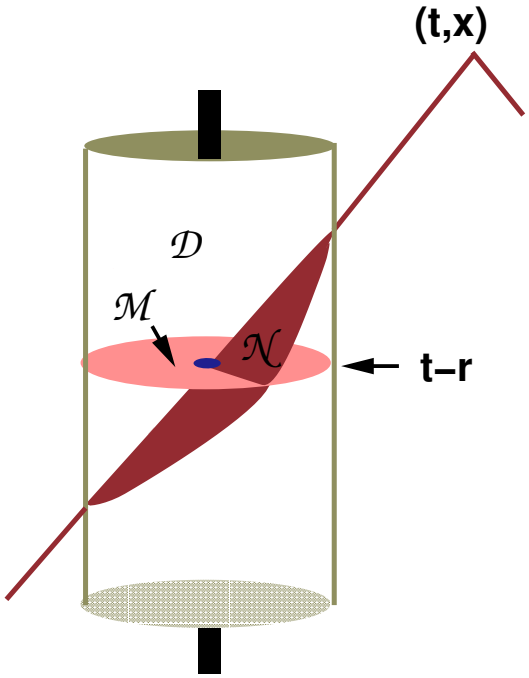

Fig. 8. Taylor expansion of retarded time dependence on $\mathcal{N}$ results in multipole moments integrated over the spatial hypersurface $\mathcal{M}$, corresponding to fixed retarded time $t - r$

solution is a *retarded* integral, *i.e.* an integral over the *entire* past null cone of the field point.[51] To be sure, that part of the integral that extends over the intersection $\mathcal{N}$ between the past null cone and the material source and the near zone is still approximated as usual by a slow-motion expansion involving spatial integrals over $\mathcal{M}$ of moments of the source, including the non-compact gravitational contributions, just as in the BDI framework (Fig. 8). But instead of cavalierly extending the spatial integrals to infinity as was implicit in the original EW framework, and risking undefined or divergent integrals, we terminate the integrals at the boundary of the near zone, chosen to be at a radius $\mathcal{R}$ given roughly by one wavelength of the gravitational radiation. For the integral over the rest of the past null cone exterior to the near zone ("radiation zone"), we neither make a slow-motion expansion nor continue to integrate over a spatial hypersurface, instead we use a coordinate transformation in the integral from the spatial coordinates d^3x' to quasi-null coordinates du', $d\theta'$, $d\phi'$, where

$$t - u' = r' + |\mathbf{x} - \mathbf{x}'| \,, \tag{70}$$

to convert the integral into a convenient, easy-to-calculate form, that is manifestly convergent, subject only to reasonable assumptions about the past behavior of the source:

$$h^{\alpha\beta}_{\mathcal{C}-\mathcal{N}}(t,x) = 4\int_{-\infty}^{u} du' \int \frac{\tau^{\alpha\beta}(u'+r',\mathbf{x}')}{t-u'-\mathbf{n}'\cdot\mathbf{x}}[r'(u',\Omega')]^2 d^2\Omega' \,. \tag{71}$$

This transformation was suggested by earlier work on a non-linear gravitational-wave phenomenon called the Christodoulou memory.[52] Not only are all integrations now explicitly finite and convergent, one can show that all contributions from the finite, near-zone spatial integrals that depend upon $\mathcal{R}$ are actually *cancelled* by corresponding terms from the radiation-zone integrals, valid for both positive and negative powers of $\mathcal{R}$ and for terms logarithmic in $\mathcal{R}$.[53] Thus the procedure, as expected, has no dependence on the artificially chosen boundary radius $\mathcal{R}$ of the near-zone. In addition, the method can be carried to higher orders in a straightforward manner. The result is a manifestly finite, well-defined procedure for calculating gravitational radiation to high orders.

The result of the DIRE or BDI calculations is an explicit formula for two-body systems in general orbits, for the transverse-traceless (TT) part of the radiation-zone field, denoted h^{ij}, and representing the deviation of the metric from flat spacetime. In terms of an expansion beyond the quadrupole formula, it has the

schematic form,

$$h^{ij} = \frac{2G\mu}{R}\left\{\tilde{Q}^{ij}[1 + O(\epsilon^{1/2}) + O(\epsilon) + O(\epsilon^{3/2}) + O(\epsilon^2)\ldots]\right\}_{TT} , \qquad (72)$$

where μ is the reduced mass, R is the distance to the source, and $\tilde{Q}^{ij}$ represents two time derivatives of the mass quadrupole moment tensor (the series actually contains multipole orders beyond quadrupole). The expansion parameter ϵ is related to the orbital variables by $\epsilon \sim m/r \sim v^2$, where r is the distance between the bodies, v is the relative velocity, and $m = m_1 + m_2$ is the total mass ($G = c = 1$). The 1/2PN and 1PN terms were derived by Wagoner and Will,[49] the 3/2PN terms by Wiseman.[50] The contribution of gravitational-wave "tails", caused by backscatter of the outgoing radiation off the background spacetime curvature, at $O(\epsilon^{3/2})$, were derived and studied by several authors. The 2PN terms including 2PN tail contributions were derived by two independent groups and are in complete agreement (see Refs. 51,54 for details and references to earlier work).

There are also contributions to the waveform due to intrinsic spin of the bodies, which occur at $O(\epsilon^{3/2})$ (spin-orbit) and $O(\epsilon^2)$ (spin-spin); these have been calculated elsewhere.[55]

Given the gravitational waveform, one can compute the rate at which energy is carried off by the radiation (schematically $\int \dot{h}\dot{h}d\Omega$, the gravitational analog of the Poynting flux). For the special case of non-spinning bodies moving on quasi-circular orbits (*i.e.* circular apart from a slow inspiral), the energy flux through 2PN order has the form

$$\begin{aligned}\frac{dE}{dt} &= \frac{32}{5}\eta^2\left(\frac{m}{r}\right)^5\left[1 - \frac{m}{r}\left(\frac{2927}{336} + \frac{5}{4}\eta\right)\right. \\ &\quad \left. + 4\pi\left(\frac{m}{r}\right)^{3/2} + \left(\frac{m}{r}\right)^2\left(\frac{293383}{9072} + \frac{380}{9}\eta\right)\right] , \qquad (73)\end{aligned}$$

where $\eta = m_1 m_2/m^2$. The first term is the quadrupole contribution, the second term is the 1PN contribution, the third term, with the coefficient 4π, is the "tail" contribution, and the fourth term is the 2PN contribution first reported jointly by Blanchet *et al.*[56] Calculation of the 3PN contributions is nearing completion.

Similar expressions can be derived for the loss of angular momentum and linear momentum. These losses react back on the orbit to circularize it and cause it to inspiral. The result is that the orbital phase (and consequently the gravitational-wave phase) evolves non-linearly with time. It is the sensitivity of

the broad-band LIGO and VIRGO-type detectors to phase that makes the higher-order contributions to dE/dt so observationally relevant. A ready-to-use set of formulae for the 2PN gravitational waveform template, including the non-linear evolution of the gravitational-wave frequency (not including spin effects) have been published[57] and incorporated into the Gravitational Radiation Analysis and Simulation Package (GRASP), a publically available software toolkit.[58]

5.3 Polarization of gravitational waves

A laser-interferometric or resonant bar gravitational-wave detector measures the local components of a symmetric 3×3 tensor which is composed of the "electric" components of the Riemann tensor, R_{0i0j}. These six independent components can be expressed in terms of polarizations (modes with specific transformation properties under null rotations). Three are transverse to the direction of propagation, with two representing quadrupolar deformations and one representing a monopole "breathing" deformation. Three modes are longitudinal, with one an axially symmetric stretching mode in the propagation direction, and one quadrupolar mode in each of the two orthogonal planes containing the propagation direction. General relativity predicts only the first two transverse quadrupolar modes, independently of the source, while scalar-tensor gravitational waves can in addition contain the transverse breathing mode. More general metric theories predict up to the full complement of six modes (TEGP 10.2). A suitable array of gravitational antennas could delineate or limit the number of modes present in a given wave. The strategy depends on whether or not the source direction is known. In general there are eight unknowns (six polarizations and two direction cosines), but only six measurables (R_{0i0j}). If the direction can be established by either association of the waves with optical or other observations, or by time-of-flight measurements between separated detectors, then six suitably oriented detectors suffice to determine all six components. If the direction cannot be established, then the system is underdetermined, and no unique solution can be found. However, if one assumes that only transverse waves are present, then there are only three unknowns if the source direction is known, or five unknowns otherwise. Then the corresponding number (three or five) of detectors can determine the polarization. If distinct evidence were found of any mode other than the two transverse quadrupolar modes of GR, the result would be disastrous for GR. On the other hand, the absence of a

breathing mode would not necessarily rule out scalar-tensor gravity, because the strength of that mode depends on the nature of the source.

Although some of the details of implementing such polarization observations have been worked out for arrays of resonant cylindrical, disk-shaped, and spherical detectors (TEGP 10.2, Ref. 59) only initial work has been done to assess whether the ground-based laser-interferometers (LIGO, VIRGO, GEO600, TAMA300) could perform interesting polarization measurements. The results depend sensitively on the relative orientation of the detectors' arms, which are now cast (literally) in concrete.

5.4 Speed of gravitational waves

According to GR, in the limit in which the wavelength of gravitational waves is small compared to the radius of curvature of the background spacetime, the waves propagate along null geodesics of the background spacetime, *i.e.* they have the same speed, c, as light (henceforth, we do not set $c = 1$). In other theories, the speed could differ from c because of coupling of gravitation to "background" gravitational fields. For example, in the Rosen bimetric theory with a flat background metric $\boldsymbol{\eta}$, gravitational waves follow null geodesics of $\boldsymbol{\eta}$, while light follows null geodesics of $\mathbf{g}$ (TEGP 10.1).

Another way in which the speed of gravitational waves could differ from c is if gravitation were propagated by a massive field (a massive graviton), in which case, v_g would be given by, in a local inertial frame,

$$\frac{v_g^2}{c^2} = 1 - \frac{m_g^2 c^4}{E^2}\,, \tag{74}$$

where m_g and E are the graviton rest mass and energy, respectively. For a recent review of the idea of a massive graviton see Ref. 60.

The most obvious way to test this is to compare the arrival times of a gravitational wave and an electromagnetic wave from the same event, *e.g.* a supernova. For a source at a distance D, the resulting value of the difference $1 - v_g/c$ is

$$1 - \frac{v_g}{c} = 5 \times 10^{-17} \left(\frac{200\mathrm{Mpc}}{D}\right) \left(\frac{\Delta t}{1\mathrm{s}}\right)\,, \tag{75}$$

where $\Delta t \equiv \Delta t_a - (1+Z)\Delta t_e$ is the "time difference", where Δt_a and Δt_e are the differences in arrival time and emission time, respectively, of the two signals, and Z is the redshift of the source. In many cases, Δt_e is unknown, so that the best

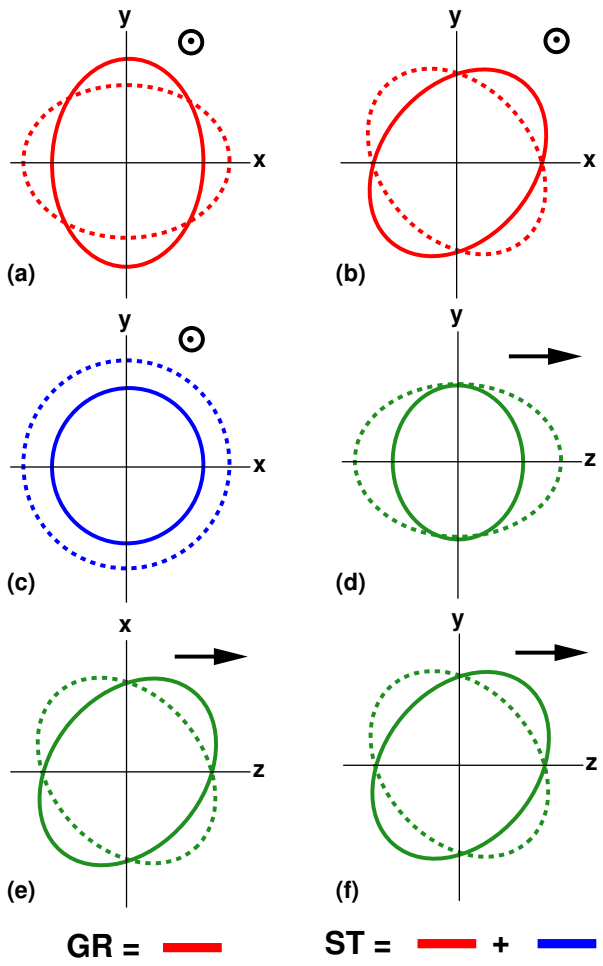

Fig. 9. Six polarization modes for gravitational waves permitted in any metric theory of gravity. Shown is the displacement that each mode induces on a ring of test particles. The wave propagates in the $+z$ direction. There is no displacement out of the plane of the picture. In (a), (b) and (c), the wave propagates out of the plane; in (d), (e), and (f), the wave propagates in the plane. In general relativity, only (a) and (b) are present; in scalar-tensor gravity, (c) may also be present.

one can do is employ an upper bound on Δt_e based on observation or modelling. The result will then be a bound on $1 - v_g/c$.

For a massive graviton, if the frequency of the gravitational waves is such that $hf \gg m_g c^2$, where h is Planck's constant, then $v_g/c \approx 1 - \frac{1}{2}(c/\lambda_g f)^2$, where $\lambda_g = h/m_g c$ is the graviton Compton wavelength, and the bound on $1 - v_g/c$ can be converted to a bound on λ_g, given by

$$\lambda_g > 3 \times 10^{12} \text{ km} \left(\frac{D}{200 \text{ Mpc}} \frac{100 \text{ Hz}}{f}\right)^{1/2} \left(\frac{1}{f\Delta t}\right)^{1/2} . \tag{76}$$

The foregoing discussion assumes that the source emits *both* gravitational and electromagnetic radiation in detectable amounts, and that the relative time of emission can be established to sufficient accuracy, or can be shown to be sufficiently small.

However, there is a situation in which a bound on the graviton mass can be set using gravitational radiation alone.[61] That is the case of the inspiralling compact binary. Because the frequency of the gravitational radiation sweeps from low frequency at the initial moment of observation to higher frequency at the final moment, the speed of the gravitons emitted will vary, from lower speeds initially to higher speeds (closer to c) at the end. This will cause a distortion of the observed phasing of the waves and result in a shorter than expected overall time Δt_a of passage of a given number of cycles. Furthermore, through the technique of matched filtering, the parameters of the compact binary can be measured accurately, (assuming that GR is a good approximation to the orbital evolution, even in the presence of a massive graviton), and thereby the emission time Δt_e can be determined accurately. Roughly speaking, the "phase interval" $f\Delta t$ in Eq. (76) can be measured to an accuracy $1/\rho$, where ρ is the signal-to-noise ratio.

Thus one can estimate the bounds on λ_g achievable for various compact inspiral systems, and for various detectors. For stellar-mass inspiral (neutron stars or black holes) observed by the LIGO/VIRGO class of ground-based interferometers, $D \approx 200$Mpc, $f \approx 100$Hz, and $f\Delta t \sim \rho^{-1} \approx 1/10$. The result is $\lambda_g > 10^{13}$km. For supermassive binary black holes (10^4 to $10^7 M_\odot$) observed by the proposed laser-interferometer space antenna (LISA), $D \approx 3$Gpc, $f \approx 10^{-3}$Hz, and $f\Delta t \sim \rho^{-1} \approx 1/1000$. The result is $\lambda_g > 10^{17}$ km.

A full noise analysis using proposed noise curves for the advanced LIGO and for LISA weakens these crude bounds by factors between two and 10. These

potential bounds can be compared with the solid bound $\lambda_g > 2.8 \times 10^{12}$ km, derived from solar system dynamics, which limit the presence of a Yukawa modification of Newtonian gravity of the form $V(r) = (GM/r)\exp(-r/\lambda_g)$,[62] and with the model-dependent bound $\lambda_g > 6 \times 10^{19}$ km from consideration of galactic and cluster dynamics.[60]

5.5 Gravitational Radiation Back-reaction

This plays an important role only in the inspiral of compact objects. The equations of motion of inspiral include the non-radiative, non-linear post-Newtonian corrections of Newtonian motion, as well as radiation back-reaction and its non-linear post-Newtonian corrections. The evolution of the orbit is imprinted on the phasing of the inspiral waveform, to which broad-band laser interferometers are especially sensitive through the use of matched filtering of the data against theoretical templates derived from GR.[63] A number of tests of GR using matched filtering of binary inspiral have been discussed, including putting a bound on scalar-tensor gravity,[64] measuring the non-linear "tail term" in gravitational radiation damping[65] (the "4π" term in Eq. (73)), and testing the GR "no hair" theorems by mapping spacetime outside black holes.[66]

For example, the dipole gravitational radiation predicted by scalar-tensor theories results in modifications in gravitational-radiation back-reaction. The effects are strongest for systems involving a neutron star and a black hole. Double neutron star systems are less promising because the small range of masses available near 1.4 $M_\odot$ results in suppression of dipole radiation by symmetry. Double black-hole systems turn out to be observationally identical in the two theories.

For example, for a 1.4 $M_\odot$ neutron star and a 10 $M_\odot$ (3 $M_\odot$) black hole at 200 Mpc, the bound on $\omega_{\rm BD}$ could be 600 (1800) (using advanced LIGO noise curves). The bound increases linearly with signal-to-noise ratio. If one demands that this test be performed annually, thus requiring observation of frequent, and therefore more distant, weaker sources, the bounds on $\omega_{\rm BD}$ will be too weak to compete with existing bounds. However, if one is prepared to wait 10 years for the lucky observation of a nearby, strong source, the resulting bound could exceed the current bound. The bounds are illustrated in Figure 10 by the curves marked $N = 1$ and $N = 1/10$. Figure 10 assumes a double-neutron-star inspiral rate of 10^{-6} per year per galaxy, and a black-hole-neutron-star rate β times that, where

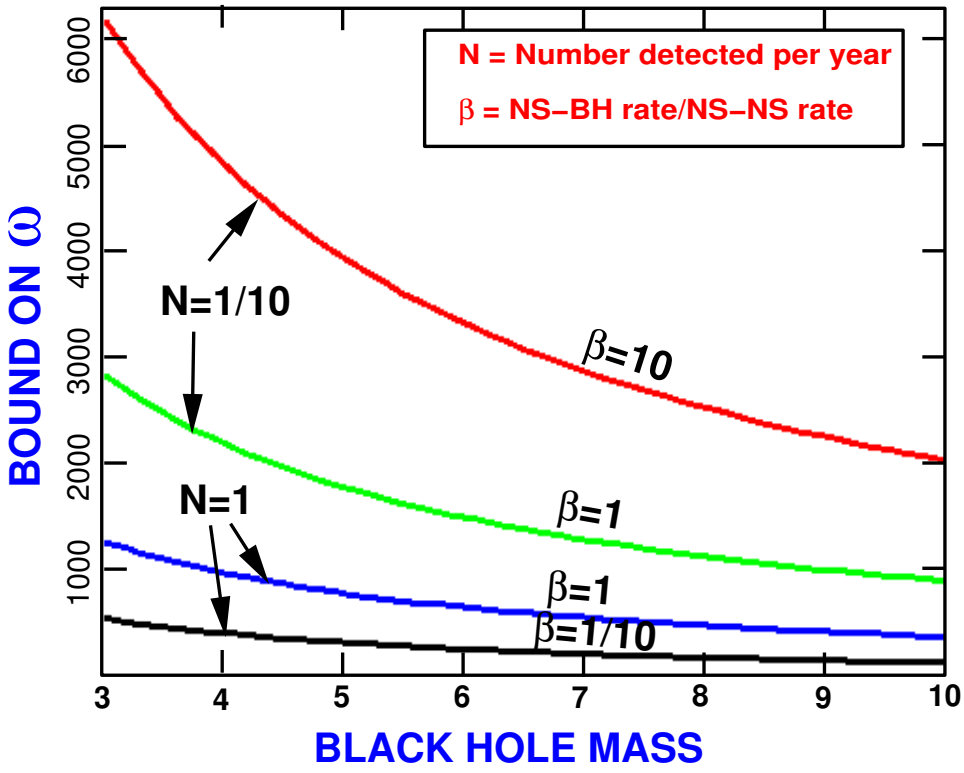

Fig. 10. Bounds on the scalar-tensor coupling constant $\omega_{\rm BD}$ from gravitational-wave observations of inspiralling black-hole neutron-star systems. The solar system bound is around $\omega_{\rm BD} = 3000$.

β is highly uncertain.

6 Conclusions

In 1998 we find that general relativity has held up under extensive experimental scrutiny. The question then arises, why bother to continue to test it? One reason is that gravity is a fundamental interaction of nature, and as such requires the most solid empirical underpinning we can provide. Another is that all attempts to quantize gravity and to unify it with the other forces suggest that the standard general relativity of Einstein is not likely to be the last word. Furthermore, the predictions of general relativity are fixed; the theory contains no adjustable constants so nothing can be changed. Thus every test of the theory is either a

potentially deadly test or a possible probe for new physics. Although it is remarkable that this theory, born 80 years ago out of almost pure thought, has managed to survive every test, the possibility of finding a discrepancy will continue to drive experiments for years to come.

Acknowledgments

This work was supported in part by the National Science Foundation, Grant Number PHY 96-00049.

References

[1] C. M. Will *Was Einstein Right?* 2nd Ed. (Basic Books, New York, 1993).

[2] C. M. Will, *Theory and Experiment in Gravitational Physics* 2nd Ed. (Cambridge University Press, Cambridge, 1993).

[3] C. M. Will, in *300 Years of Gravitation*, edited by S. W. Hawking and W. Israel, 80–127 (Cambridge University Press, Cambridge, 1987), p. 80.

[4] C. M. Will, Int J. Mod. Phys. D **1**, 13 (1992).

[5] C. M. Will, in *General Relativity: Proceedings of the 46th Scottish Universities Summer School in Physics*, ed. G. S. Hall and J. R. Pulham (Institute of Physics Publishing, Bristol, 1996), p. 239.

[6] T. Damour, in *Proceedings of the 5th Hellenic School on Elementary Particle Physics*, in press (gr-qc/9606079).

[7] Y. Su, B. R. Heckel, E. G. Adelberger, J. H. Gundlach, M. Harris, G. L. Smith, and H. E. Swanson, Phys. Rev. D **50**, 3614 (1994).

[8] E. Fischbach, G. T. Gillies, D. E. Krause, J. G. Schwan, and C. Talmadge, Metrologia **29**, 213 (1992).

[9] A. Godone, C. Novero, and P. Tavella, Phys. Rev. D **51**, 319 (1995).

[10] J. D. Prestage, R. L. Tjoelker, and L. Maleki, Phys. Rev. Lett. **74**, 3511 (1995).

[11] F. Dyson and T. Damour, Nucl. Phys. **B480**, 37 (1996) (hep-ph/9606486).

[12] M. J. Drinkwater, J. K. Webb, J. D. Barrow, and V. V. Flambaum, Mon. Not. R. Astron. Soc. **295**, 457 (1998) (astro-ph/9711290).

[13] R. A. Malaney and G. Mathews, Phys. Rep. **229**, 147 (1993); H. Reeves, Rev. Mod. Phys. **66**, 193 (1994).

[14] C. M. Will, Phys. Rev. D **45** 403 (1992).

[15] E. Fischbach and C. Talmadge, Nature **356**, 207 (1992).

[16] C. M. Will, Sky and Telescope **80**, 472 (1990).

[17] E. G. Adelberger, B. R. Heckel, C. W. Stubbs, and W. F. Rogers, Ann. Rev. Nucl. Particle Sci. **41**, 269 (1991).

[18] C. W. Misner, K. S. Thorne, and J. A. Wheeler, *Gravitation* (Freeman Publishing Co, San Francisco, 1973).

[19] S. W. Weinberg S W, *Gravitation and Cosmology* (Wiley, New York, 1992).

[20] T. Damour and G. Esposito-Farèse, Class. Quantum Grav. **9**, 2093 (1992).

[21] T. Damour and K. Nordtvedt, Phys. Rev. Lett. **70**, 2217 (1993); Phys. Rev. D **48**, 3436 (1993).

[22] P. J. Steinhardt and C. M. Will, Phys. Rev. D **52**, 628 (1995) (astro-ph/9409041).

[23] T. Damour and G. Esposito-Farèse, Phys.Rev. D **54**, 1474 (1996) (gr-qc/9602056).

[24] T. M. Eubanks, D. N. Matsakis, J. O. Martin, B. A. Archinal, D. D. McCarthy, S. A. Klioner, S. Shapiro, and I. I. Shapiro, Bull. Am. Phys. Soc., Abstract #K 11.05 (1997), unpublished

[25] M. Froeschlé, F. Mignard and F. Arenou, in *Proceedings of the Hipparcos Venice 1997 Symposium*, in press.

[26] K. Nordtvedt, Icarus **114**, 51 (1995).

[27] T. Damour and D. Vokrouhlický, Phys. Rev. D, **53**, 6740 (1996) (gr-qc/9606076).

[28] J. O. Dickey, P. L. Bender, J. E. Faller, X X Newhall, R. L. Ricklefs, J. G. Ries, P. J. Shelus, C. Veillet, A. L. Whipple, J. R. Wiant, J. G. Williams, and C. F. Yoder, Science **265**, 482 (1994); J. G. Williams, X X Newhall, and J. O. Dickey, Phys. Rev. D**53**, 6730 (1996).

[29] J. F. Bell and T. Damour, Class. Quantum Grav. **13**, 3121 (1996) (gr-qc/9606062).

[30] J. F. Bell, F. Camilo, T. Damour, Astrophys. J. **464**, 857 (1996) (astro-ph/9512100).

[31] C. M. Will, Astrophys J **204**, 224 (1976).

[32] C. M. Will, Astrophys J. Lett. **393**, L59 (1992).

[33] For information about the project, see http://einstein.stanford.edu/.

[34] I. Ciufolini, E. Pavlis, F. Chieppa, E. Fernandes-Vieira, and J. Pirez-Mercader, Science **279**, 2100 (1998).

[35] K. S. Thorne, in *Proceedings of the Snowmass 95 Summer Study on Particle and Nuclear Astrophysics and Cosmology*, edited by E. W. Kolb and R. Peccei (World Scientific, Singapore, 1995), p. 398 (gr-qc/9506086).

[36] R. A. Hulse, Rev. Mod. Phys. **66**, 699 (1994).

[37] J. H. Taylor, Rev. Mod. Phys. **66**, 711 (1994).

[38] T. Damour , 1987, in *300 Years of Gravitation*, eds Hawking S W and Israel W, 128–198 (Cambridge University Press, Cambridge).

[39] M. Kramer, Astrophys. J., in press (astro-ph/9808127).

[40] A. Wolszczan, Class. Quantum Grav. **11**, A227 (1994).

[41] I. H. Stairs, Z. Arzoumanian, F. Camilio, A. G. Lyne, D. J. Nice, J. H. Taylor, S. E. Thorsett, and A. Wolszczan, Astrophys. J., in press (astro-ph/9712296).

[42] L. S. Finn and D. F. Chernoff, Phys. Rev. D **47**, 2198 (1993) (gr-qc/9301003); C. Cutler and É. E. Flanagan, Phys. Rev. D **49**, 2658 (1994) (gr-qc/9402014); E. Poisson and C. M. Will, Phys. Rev. D **52**, 848 (1995) (gr-qc/9502040).

[43] This convention holds sway, despite the fact that pure Newtonian gravity predicts no gravitational radiation. It is often the source of confusion, since the energy carried by the lowest-order "Newtonian" quadrupole radiation manifests itself in a $(\text{post})^{5/2}$-Newtonian, or $O[(v/c)^5]$ correction in the equation of motion.

[44] M. Walker and C. M. Will, Phys. Rev. Lett. **45**, 1741 (1980); J. L. Anderson, Phys. Rev. Lett. **45**, 1745 (1980); T. Damour, Phys. Rev. Lett. **51**, 1019 (1983); D. Christodoulou and B. G. Schmidt, Commun. Math. Phys. **68**, 275 (1979); R. A. Isaacson, J. S. Welling, and J. Winicour, Phys. Rev. Lett. **53**, 1870 (1984).

[45] L. Blanchet, T. Damour, Phil. Trans. R. Soc. London **A320**, 379 (1986); L. Blanchet and T. Damour, Phys. Rev. D **37**, 1410 (1988); L. Blanchet and T. Damour, Ann. Inst. H. Poincaré (Phys. Theorique) **50**, 377 (1989); T. Damour and B. R. Iyer, Ann. Inst. H. Poincaré (Phys. Theorique) **54**, 115 (1991); L. Blanchet, Phys. Rev. D **51**, 2559 (1995) (gr-qc/9501030); L. Blanchet and T. Damour, Phys. Rev. D **46**, 4304 (1992).

[46] K. S. Thorne, Rev. Mod. Phys. **52**, 299 (1980).

[47] R. Epstein and R. V. Wagoner, Astrophys. J. **197**, 717 (1975) (EW).

[48] E. Poisson, Phys. Rev. D **47**, 1497 (1993); E. Poisson and M. Sasaki, Phys. Rev. D **51**, 5753 (1995) (gr-qc/9412027); C. Cutler, L. S. Finn, E. Poisson, and G. J. Sussman, Phys. Rev. D **47**, 1511 (1993); M. Sasaki, Prog. Theor. Phys. **92**, 17 (1994) (gr-qc/9402042); H. Tagoshi and M. Sasaki, Prog. Theor. Phys. **92**, 745 (1994) (gr-qc/9405062); T. Tanaka, H. Tagoshi, and M. Sasaki, Prog. Theor. Phys. **96**, 1087 (1996) (gr-qc/9701050).

[49] R. V. Wagoner and C. M. Will, Astrophys. J. **210**, 764 (1976).

[50] A. G. Wiseman, Phys. Rev. D **46** 1517 (1992).

[51] C. M. Will and A. G. Wiseman, Phys. Rev. D **54**, 4813 (1996) (gr-qc/9608012).

[52] A. G. Wiseman and C. M. Will, Phys. Rev. D **44**, R2945 (1991).

[53] C. M. Will and M. E. Pati, papers in preparation.

[54] L. Blanchet, T. Damour, and B. R. Iyer, Phys. Rev. D **51**, 5360 (1995) (gr-qc/9501029).

[55] L. E. Kidder, C. M. Will, and A. G. Wiseman, Phys. Rev. D **47**, R4183 (1993) (gr-qc/9211025); L. E. Kidder, Phys. Rev. D **52**, 821 (1995) (gr-qc/9506022).

[56] L. Blanchet, T. Damour, B. R. Iyer, C. M. Will and A. G. Wiseman, Phys. Rev. Lett. **74**, 3515 (1995) (gr-qc/9501027).

[57] L. Blanchet, B. R. Iyer, C. M. Will, and A. G. Wiseman, Class. Quantum Grav. **13**, 575 (1996) (gr-qc/9602024).

[58] See http://www.ligo.caltech.edu/LIGO_web/Collaboration/manual.pdf.

[59] J. A. Lobo, Phys. Rev. D**52**, 591 (1995).

[60] M. Visser, Gen. Relativ. Gravit., in press (gr-qc/9705051).

[61] C. M. Will, Phys. Rev. D**57**, 2061 (1998) (gr-qc/9709011).

[62] C. Talmadge, J.-P. Berthias, R. W. Hellings, and E. M. Standish, Phys. Rev. Lett. **61**, 1159 (1988).

[63] C. Cutler, T. A. Apostolatos, L. Bildsten, L. S. Finn, É. E. Flanagan, D. Kennefick, D. M. Marković, A. Ori, E. Poisson, G. J. Sussman, and K. S. Thorne, Phys. Rev. Lett. **70**, 2984 (1993) (astro-ph/9208005).

[64] C. M. Will, Phys. Rev. D**50** 6058 (1994) (gr-qc/9406022).

[65] L. Blanchet and B. S. Sathyaprakash, Class. Quantum Grav. **11**, 2807 (1994); Phys. Rev. Lett. **74**, 1067 (1995).

[66] F. D. Ryan, Phys. Rev. D**52**, 5707 (1995); E. Poisson, Phys. Rev. D**54**, 5939 (1996) (gr-qc/9606024).